Assessing Bioimpedance as a Method for Determining Ischemia-Reperfusion Injury in Marginalised Livers during Machine Perfusion

Mellie M Livingston

Thesis submitted for the degree of Master of Science
in Electrical Engineering, Informatics and Technology:
Microelectronics and Sensor Technology
60 credits

Department of Physics
Faculty of Mathematics and Natural Sciences

UNIVERSITY OF OSLO

Spring 2021

II

Assessing Bioimpedance as a Method for Determining Ischemia-Reperfusion Injury in Marginalised Livers during Machine Perfusion

Mellie M Livingston

Assessing Bioimpedance as a Method for Determining Ischemia-Reperfusion Injury in Marginalised Livers during Machine Perfusion

IV

Abstract

Over the past 20 years a steady increase in the waiting list for liver transplantations has been reported in the Nordic countries. To increase the donor pool, donor organ criteria has been extended to include donation after circulatory death (DCD) which has been associated with ischemia-reperfusion related injuries (IRI). In recent years, machine perfusion has become a rapidly advancing technology, gaining popularity in replacing cold storage organ preservation prior to transplantation. Currently, the standard assessment of liver viability is based on subjective visual inspection and patient history. To reduce uncertainty of liver viability, development of new methods to aid the surgeon in assessment of marginalised livers upon reperfusion is imperative. Bioimpedance measures changes in electrical parameters correlating to changes in cell structures within biological tissue and has been applied in a multitude of studies in assessment of ischemia. The aim of this study is to assess bioimpedance as a method to determine the level of IRI displayed by marginalised livers upon machine perfusion.

A total of 16 experiments were conducted on porcine liver, including pilot experiments, with statistical analysis collected from 12 experiments. The 12 experiments were divided into three models: control, biliary injury (partial warm ischemia) and static cold storage (overall liver injury). Trans-lobe measurements were conducted in-vivo and upon machine perfusion using Ag/AgCl two-electrode setup connected to Solartron 1260A Impedance/Gain-phase Analyzer with a 1294 Solartron Impedance Interface.

Trans-lobe bioimpedance measurements in the biliary injury model did not predict partial liver hypoxia compared to the control group, as we believe the liver parenchyma received sufficient blood flow from the portal vein during occlusion of the hepatic artery. Significant differences in the time-development of passive electrical properties were found between static cold storage and control livers, with ($P < 0.01$) in phase angle (φ) and loss tangent ($\tan\delta$) at low frequencies (< 800 Hz) in the two first hours of reperfusion. Given that we know the time of liver explantation, bioimpedance measurements can be utilized to discriminate the state of the liver in the intervals where the differences between the groups are deemed significant. Based on the current bioimpedance data we cannot predict irreversible effects of IRI in the marginalised liver models at the end of normothermic machine perfusion.

Acknowledgements

I want to thank my supervisor Jan Olav Høgetveit for sharing your knowledge on medical instrumentation so eloquently, further fuelling my passion for the field. Jan Olav introduced me to this project and has shown me support and guidance throughout this thesis for which I am very grateful.

To my co-supervisor Runar Strand-Amundsen, your guidance throughout these experiments has been invaluable. Your knowledge and passion for bioimpedance combined with your capacity and compassion inspire me. Thank you for your accessibility and patience, I am grateful for all I have gotten to learn from you.

To the rest of the project team, Søren E Pischke, Jie Hou, Olav M Liavåg, Ida H Færden and Tor Inge Tønnessen; working alongside you all has been a true joy. Thank you for sharing your knowledge with me and laughing at my jokes in the late evening hours.

Finally, a big thank you to my husband Hamish for endless encouragement, quick wit, dance moves, patience, and the many dinners offered during long nights working from home. You're a good egg.

Contents

List of Tables

List of Figures

List of Abbreviations

DCD   Donation after Circulatory Death

IRI   Ischemia-Reperfusion Injury

NMP   Normothermic Machine Perfusion

DHOPE   Dual Hypothermic Oxygenated Machine Perfusion

COR   Controlled Oxygenated Rewarming

SCS   Static Cold Storage

AC   Alternating Current

CPE   Constant Phase Element

EPI   Electrode Polarization Impedance

CC   Current Carrying

PU   Pick-up

CMRR   Common Mode Rejection Ratio

ROS   Reactive Oxygen-Species

ADC   Analogue to Digital Converter

SD   Standard Deviation

CI   Confidence Interval

ANOVA   Analysis of Variance

Chapter 1: Introduction

The waiting list for liver transplantations has been steadily increasing in the Nordic countries over the past 20 years. In 2020, the Nordic Liver Transplant Registry reported 404 new patients on the waiting list, whilst 360 patients received a first-time liver graft and 55 patients received a re-transplantation (Melum, 2020). Due to the high mortality rate among patients waiting for a new donor organ, donation after circulatory death (DCD) was legalized in Norway in 2009, where previously donation after brain death was the determining criteria for donation. However, DCD livers transplantations, which are subjected to warm ischemia while awaiting circulatory death, have been associated with complications from ischemia-reperfusion injury (IRI) such as ischemic cholangiopathy (Hagness et al., 2019). In order to slow down cell metabolism, the standard procedure post hepatectomy is static cold storage (SCS), however the method poses further risk of IRI during transplantation due to oxygen deprivation and accumulation of anaerobic metabolism by-products (Mergental et al., 2020; Williams & Markmann, 2021). Currently, the standard assessment of a donor liver is a subjective assessment by the surgeon, therefore marginal livers have a high chance of being discarded predominately based on visual inspection and patient history (Mergental et al., 2020). The rule of thumb if the surgeon is unsure of the liver's viability is to discard the organ. To reduce uncertainty with respect to liver viability, there is a need to introduce further testing to eliminate primary-non-function livers and livers with early signs of liver failure upon reperfusion (Hagness et al., 2019; Mergental et al., 2020).

In recent years the use of machine perfusion has been extensively researched as an alternative to SCS, and the technology is gaining popularity and is advancing rapidly. The normothermic perfusion (NMP) method allows for further assessment on whether a potentially transplantable marginalised liver can be utilised. NMP allows the liver to maintain normal metabolic activity at physiological temperatures and pressures whilst being supplied oxygen and nutrients (Mergental et al., 2020). Recent studies indicate that performing dual hypothermic oxygenated machine perfusion (DHOPE) followed by one hour controlled oxygenated rewarming (COR) prior to NMP, lowers the risk of IRI upon reperfusion (van Leeuwen, de Vries, de Meijer, & Porte, 2021). Based on these principles, a normothermic perfusion machine, following the

DHOPE-COR-NMP protocol, is currently used in a trial at Oslo University Hospital with porcine livers. Several recent studies have been conducted to investigate a variety of biomarkers in assessing liver grafts during machine perfusion. Such biomarkers include analysis of biliary parameters, perfusate pH and portal venous and hepatic artery flow (Czigany et al., 2020). Another recent study has discovered a new mitochondrial marker using spectroscopy providing real time results in the DHOPE stage as a potential new method for predicting IRI in liver grafts (Muller et al., 2019). Establishing methods for viability assessment and surveillance using biomedical technology can aid clinicians in decision making when assessing a marginalised liver upon reperfusion.

This project is part of the DHOPE-COR-NMP trial at Oslo University Hospital and aims to investigate electrical bioimpedance as a potential method to determine the state of the liver tissue upon reperfusion. Bioimpedance is the ability of a tissue to oppose a flow of alternating electric current. The electrical properties of biological tissue change dependent on the state of the tissue. During ischemia, bioimpedance parameters change due to biological processes causing changes in intra- and extracellular volume and membrane capacitance within the tissue. In addition, the vascular permeability of the tissues and the tissue structures change. Due to several factors, excised tissue can oppose the flow of electrical current differently than in-vivo tissue. The aim of ex-vivo reperfusion is to reverse the ischemic processes by returning the presence of oxygen, while trying to avoid severe reperfusion injury. Exploring the electrical properties of liver tissue in assessment of IRI, when using machine perfusion, has the potential of being a valuable tool in determining liver viability in the future.

A multitude of studies have applied bioimpedance as a non-invasive technology to assess organ state. In relation to ischemic tissue state, Gersing (1998) investigated the time-development of the impedance modulus in excised porcine liver tissue. In 2005, liver cell viability during in-vivo ischemia-reperfusion in rat livers was investigated, with need for further studies to assess the relationship between bioimpedance and liver viability (Ahn, Shin, Yun, Kim, & Choi, 2005). More recently, Strand-Amundsen et al. (2018) established the time-development of bioimpedance parameter $\tan\delta$ to be significant for detecting ischemia-reperfusion changes in porcine small intestine in-vivo. To the best of our knowledge, no studies have been published investigating bioimpedance further as a method for ischemia-reperfusion detection in liver using normothermic machine perfusion.

1.1 Aim and Objectives

As increasing the donor liver pool is important in order to reduce the waiting list for liver transplantation, the development of new methods to aid surgeons in assessing the viability of marginalised donor organs upon reperfusion is imperative (Mergental et al., 2020). The aim of this study is to assess bioimpedance as a non-invasive method to determine the level of IRI displayed by marginalised livers upon machine perfusion.

Chapter 2: Theoretical Background

2.1 General Introduction to Electrical Bioimpedance

U	Voltage [V]
I	Current [A]
R	Resistance, real part of impedance [Ω]
X	Reactance, imaginary part of impedance [Ω]
X_L	Inductive part of reactance [Ω]
X_C	Capacitive part of reactance [Ω]
Z	Impedance [Ω]
|Z|	Impedance modulus [Ω]
j	Imaginary unit, $j^2 = -1$
φ	Phase angle [deg] [rad]
tanδ	Loss tangent
tanδm	Maximum tanδ amplitude over a frequency range
R_I	Intracellular resistance [Ω]
R_E	Extracellular resistance [Ω]
C_M	Cell membrane capacitance [F]
ω	Angular frequency (2πf) [rad/s]
ε'$_r$	Lossy relative permittivity [F/m]
σ′	In-phase conductivity [S/m]
τ	Time constant
R_0	Low frequency resistance [Ω]
R∞	High frequency resistance [Ω]
α	Positive exponent constant ($0 \leq \alpha \leq 1$)

Table 1.1: Bioimpedance notation

When a current is applied to a biological material, dependent on the frequency and the amplitude of the signal, a current can pass through the material. When a current move through tissue, and impedance is measured over a range of frequencies, the ratio between voltage and current will be affected by the cellular structure of the tissue. Impedance (Z) is derived from Ohm's law and can for an alternating current (AC) be simplified to:

$$Z = \frac{U}{I} \ [\Omega] \tag{2.1}$$

where *U* is the applied voltage, and *I* is the current measured in ampere. Impedance is a complex number composed of a real part, resistance (R), and an imaginary part, reactance (X). Ideal resistance is constant regardless of the frequency, whilst reactance varies with frequency as it also takes into account the effects of opposition of capacitance and inductance to the current,

causing a phase-shift. Reactance (X) can be either inductive (X_L) or capacitive ($-X_C$). Consequently, reactance and resistance must be added as vectors to determine the right phase angle to magnitude of the impedance modulus (|Z|). The complex form of impedance is defined as:

$$Z = R + jX \quad [\Omega] \tag{2.2}$$

$$|Z| = \sqrt{R^2 + X^2} = \sqrt{R^2 + (X_L - X_C)^2} \quad [\Omega] \tag{2.3}$$

The phase-shift is due to a time delay between the voltage and current when energy is stored as reactance, causing a voltage drop which is between 0° and 90° out of phase with the current. The phase angle is proportional to the tendency of the medium to behave as an inductor or a capacitor, indicated by the sign of the phase (see Fig. 2.1). The phase angle associated with the impedance in an AC circuit is mathematically defined as:

$$\varphi = \tan^{-1}\left(\frac{X}{R}\right) \quad [\text{rad}] \tag{2.4}$$
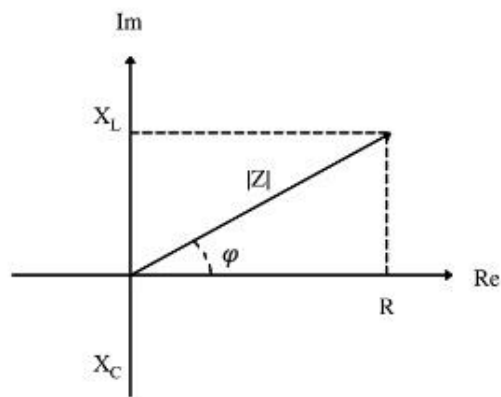
Figure 2.1: *Plot of the complex plane of impedance with resistance (R), reactance (X_L or X_C) and phase angle (φ)*

Inversely proportional to φ is the dissipation factor or loss tangent known as tanδ. R is an equivalent series resistance describing the sum of ohmic losses caused by factors such as the materials, dielectric, leads and connections. The ratio between R and the capacitive components of the reactance, X_C, produces the loss tangent tanδ. Tanδ is described as "the energy lost per

cycle divided by the energy stored per cycle" (S. Grimnes & Martinsen, 2017) which gives an indication of a dielectric affinity to absorb energy when an alternating current is externally applied to the dielectric. R is the in-phase electrical parameter which is larger than X which is an out-of-phase parameter, however the out-of-phase current dominates in biological tissue together with the conductive properties of the cells and polarization of the cell membranes (S. Grimnes & Martinsen, 2017). The dielectric loss rate of complex impedance has been reported to be a relevant parameter in assessment of ischemia and IRI in porcine small intestine as it amplifies the capacitive components of the denominator X which has been found to be sensitive to ischemic changes in tissue (Strand-Amundsen et al., 2018). Tanδ is defined as:

$$Tan\delta = \frac{R}{X} \quad \text{[dimensionless]} \tag{2.5}$$

2.1.1 Passive Electrical Properties of Tissue

Bioimpedance encompasses the passive electrical properties of tissue where we find capacitive and resistive properties in relation to the cell membranes and intra- and extracellular fluids (S. Grimnes & Martinsen, 2017). The cell membrane itself separates the intracellular and extracellular fluids and controls the cell's permeability to ionic charges. The membrane consists of a bilayer lipid membrane which is made up of phospholipids (S. Grimnes & Martinsen, 2017). Due to the insulating quality of lipids the electric conductivity of the cell membrane itself is low. A high ratio between area to cell wall thickness results in high capacitance and therefore high membrane break down potential (>150 mV) and the frequency dependence of the permittivity of the cell membrane. While the current at low AC frequencies travel in the extracellular fluid, the current path will pass through the cell membrane at high AC frequencies due high ionic polarization causing high cell permittivity, see Figure 2.2 (S. Grimnes & Martinsen, 2017).
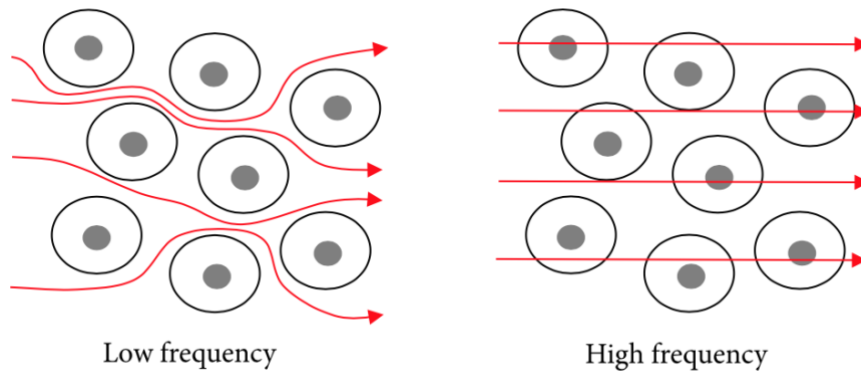
Figure 2.2: *Current path in tissue for low- and high frequency signals. (Naranjo-Hernández, Reina-Tosina, & Min, 2019)*

Tissue resistivity depends on frequency range and tissue type, and has for in-vivo and ex-vivo measurements been used to characterise parenchymal liver tissue sufficiently in the frequency range 10 Hz to 1 MHz (Haemmerich et al., 2002). Due to electrode polarization contribution being associated with the low frequency range, an area also of interest for IRI detection, we discuss the challenges surrounding this topic further in section 2.1.4.

2.1.2 Electrical Equivalent Circuit Models in Tissue

The intracellular and extracellular current paths are shown in Figure 2.3 as an equivalent circuit model of a single cell. The upper branch comprises of the cell membrane capacitance (C_M) being in series with the intracellular resistance (R_I), whilst the parallel lower branch models the current path through the extracellular resistance (R_E) (Hernández-Balaguera, López-Dolado, & Polo, 2016).
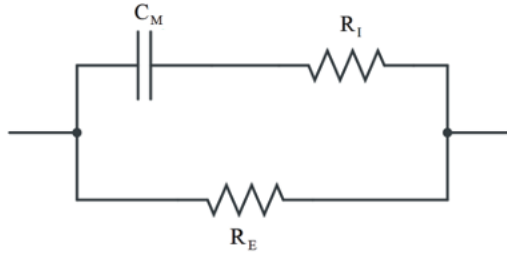
Figure 2.3: Electrical equivalent circuit model of a biological cell.

To modify the cell membrane capacitance to encompass an array of cells in tissue, C_M can be replaced with a constant phase element (CPE) which allows for the components of the electrical equivalent circuit model to be non-ideal, specifically behaving as a non-ideal capacitor or a non-ideal resistor. The elements we operate with are linear time-invariant phasors in the frequency-domain (Hernández-Balaguera et al., 2016). The electrical equivalent circuit model in Figure 2.4 demonstrates electrical behaviour of tissue in the frequency domain. The cell membrane is represented as the impedance of the membrane constant phase element $Z_{CPE_M}(j\omega)$, where j is the imaginary unit and ω is angular frequency.
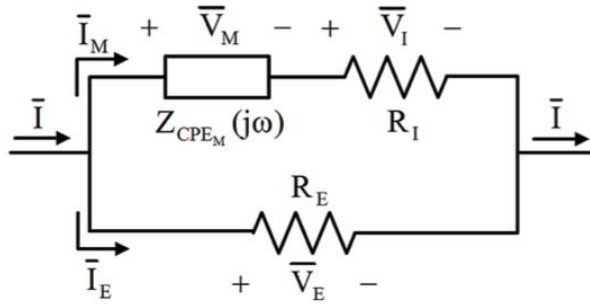
Figure 2.4: Electrical equivalent circuit model of biological tissue in frequency domain (Hernández-Balaguera et al., 2016).

To apply what we know of current paths in tissue for low- and high frequency signals at low frequencies, the current $\bar{I}$ will be approximately equal $\bar{I}_E$ due to the impedance

magnitude of $Z_{CPE_M}(j\omega)$ and R_I being much greater than R_E, giving rise to the equation $Z_{CPE_M}(j\omega) + R_I \gg R_E$. At high AC frequencies $R_I \gg Z_{CPE_M}(j\omega)$, resulting in current flowing through both R_I and R_E, as illustrated in Figure 2.2 (Hernández-Balaguera et al., 2016).

2.1.3 Dielectric Response in Tissue

Permittivity (ε) is classified as a dielectric parameter defined as the ability to store electric energy. We know from section 2.1.1 that the cell membrane's permittivity can be influenced by polarization, caused by an electrical field causing charge distributions within the medium (S. Grimnes & Martinsen, 2017). When we have an imposed AC signal the frequency will determine if charges have time to fully change their position before a new signal disturbance is introduced into the system, and therefore the degree of polarization. Permittivity and polarization will therefore decrease with increased frequency. The time between a charge disturbance and a new equilibrium for the charge is known as relaxation and occurs in the time-domain. Corresponding to relaxation theory we find dispersions, defined as permittivity as a function of frequency, in the frequency-domain (S. Grimnes & Martinsen, 2017).

Dispersions in biological tissue were first categorized by Schwan (1957) and divided into three groups: α, β and γ (S. Grimnes & Martinsen, 2017), with a fourth group, δ, being added later on. δ- and γ-dispersions appear at higher frequencies outside of the scope of this project. Each group is related to a characteristic frequency range where a range of cell related mechanisms take place. α- and β-dispersions are associated with the cell membrane, but the cellular mechanisms causing α-dispersions are not well known. It is proposed however that it is related to counter-ion polarization near the cell membrane and the surface structures of the membrane. α-dispersions can be found between 1 Hz up to 100 kHz, where as β-dispersions are found from 1 kHz to 100 MHz, see Figure 2.5 (Sverre Grimnes & Martinsen, 2010; S. Grimnes & Martinsen, 2017). β-dispersions are associated with the charge build-up at the interface between two dielectrics displaying different conductivity and permittivity parameters, also known as Maxwell-Wagner effect. Furthermore, the passive cell membrane capacitance described in section 2.1.1 takes place in this region (S. Grimnes & Martinsen, 2017).
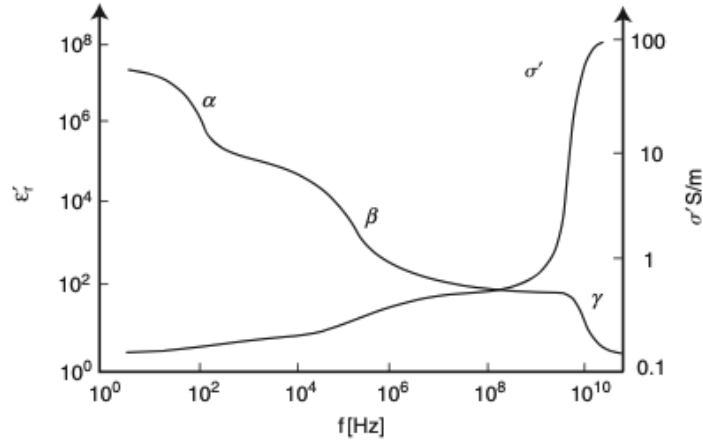
Figure 2.5: Idealized regions of dispersion in biological tissue. Complex quantities of relative permittivity(ε_r') and in-phase conductivity (σ') are plotted against frequency (S. Grimnes & Martinsen, 2017).

The Cole equation is a prevalent mathematical relaxation model used to fit bioimpedance data into a depressed arc locus in a Nyquist plot. The Cole equation is defined as:

$$Z = R\infty + \frac{R_0 - R\infty}{1 + (j\omega\tau)^\alpha} \qquad (2.6)$$

Where $R\infty$ is the high frequency resistance, R_0 is low frequency resistance, ω is the angular frequency, τ is the relaxation time constant and α is a positive constant, where $0 \leq \alpha \leq 1$ (S. Grimnes & Martinsen, 2017).

2.1.4 Electrode Polarization and Dielectric Contact

All biological tissues can be viewed as dielectrics or wet electrolytic conductors. There are several phenomena that must be accounted for that can influence the measurements. One important consideration is that of electrode polarization impedance (EPI), where effects from the interface between electrode materials and liquid can create noise that can distort low frequency measurements. To minimize contribution to EPI from

electrodes careful consideration must be taken with respect to the electrode metal, electrode setup and electrode contact area to the tissue.

A current-carrying (CC) electrode is defined a polarized electrode as current flows through it (S. Grimnes & Martinsen, 2017). When tissue with free ions is subjected to an externally applied electric field, the free ions form ionic double layers at the electrode/tissue interface. This phenomenon causes a rapid voltage decrease in these layers causing high capacitance, due to electrode resistance (R) and capacitive reactance (X_C) being is in series with the electrolytic resistance of the tissue, which can dominate at low frequencies (Ishai, Talary, Caduff, Levy, & Feldman, 2013).
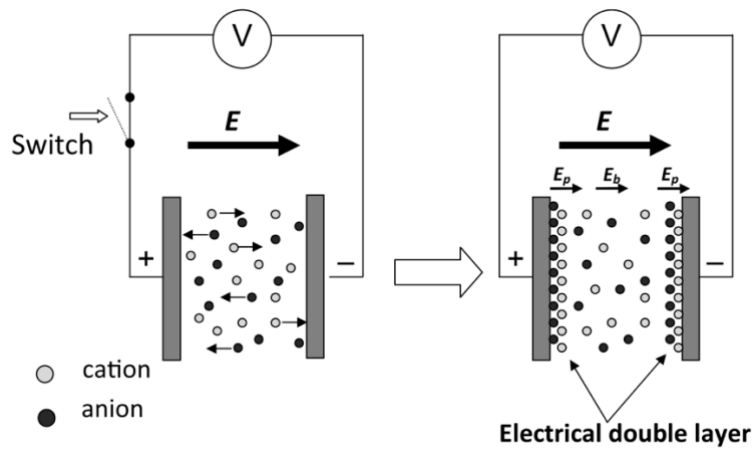
Figure 2.6: *Imposed electric field (E) resulting in ionic double layer at electrode/tissue interface causing $E = E_b + 2E_p$ where electric field from polarization will dominate over electric field from biomaterial at low frequencies (Ishai et al., 2013).*

In a four-electrode system the potential drop in EPI equals zero Ohms due to the separation of CC and pick-up (PU) electrodes (S. Grimnes & Martinsen, 2017). However, four-electrode systems are not without errors and demand extensive analysis due to decreased common mode rejection ratio (CMRR) at low frequencies and parasitic capacitances appearing at high frequencies.

A three-electrode system consists of a CC electrode, a PU (neutral reference electrode without current flow) and a measuring electrode which is both a CC and a PU electrode.

Similar to the four-electrode system, the three-electrode system measures transfer impedance. Only the measuring electrode will contribute to the EPI as transfer impedance will be measured between the measuring electrode and the PU electrode, which acts as a fixed voltage electrode (S. Grimnes & Martinsen, 2017).

In a two-electrode system where both electrodes act as CC and PU electrodes, it is important to consider the contribution from EPI and assess if there is a need for correction methods. Among the suggested correction methods we find algorithmic correction, using electrode coating, or using electrode setups such as the four-electrode system (Ishai et al., 2013).

When using a two-electrode setup, a method to reduce the effect of EPI is to increase the electrode area. The surface area between a half-spherical metal electrode and biomaterial is inversely proportional to EPI, consequently increasing the electrode contact area contributes to reducing EPI (S. Grimnes & Martinsen, 2017). A two-electrode system will only provide reliable measurements in frequency ranges where EPI is not dominating over the contribution from the electrical properties of the tissue. This depends on both the electrical properties of the tissue of interest (the lower impedance the more EPI can dominate), the electrode material, the surface structure of the electrode material, the relative positioning of the electrodes, the size of the electrodes relative to each other, and the active area of the electrodes (Miklavcic, Pavselj, & Hart, 2006). The electrode material is of interest as it determines the electric double layer. Through using a slightly soluble coating on a metal electrode, such as with non-polarizable silver-silver chloride (Ag/AgCl) electrodes, charges can cross the electrode-electrolyte barrier more readily, effectively lowering the transition impedance. To characterize a metal's EPI submersion in saline solution, having the lowest physiological impedance, can help determine what material to use as well as establishing the frequency range where EPI distorts the measurement (Albulbul, 2016).
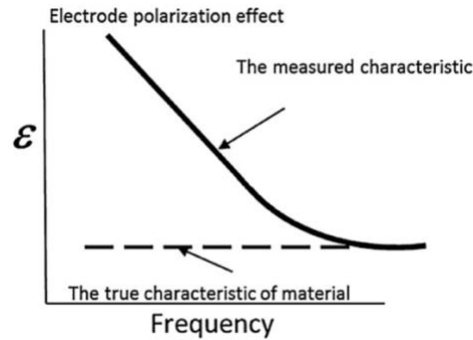
Figure 2.7: Relative permittivity vs. frequency demonstrating the electrode polarization effect (Ishai et al., 2013).

2.2 The Liver

The liver is a complex organ responsible for regulating a vast range of vital systems in the body. Functions of the liver include, but are not limited to, blood detoxification, urea and glycolytic metabolism, nutrition modulation, storage and regulating haematological and endocrine systems (Gordillo, Evans, & Gouon-Evans, 2015; Yang, 2021). It is a solid organ located inferior to the diaphragm in the upper right-hand section of the abdominal quadrant. It has dual blood supply and receives oxygen-rich blood via the hepatic artery and nutrient-rich blood via the portal vein. The contribution from the portal vein with partly oxygenated blood is the reason that the occlusion of the hepatic artery in-vivo in this project is referred to as a partial warm ischemia.

2.2.1 Structure of Liver Tissue

Measurement of electrical properties of biological tissues can be complicated due to factors such as tissue metabolism, inhomogeneity and anisotropy (Miklavcic et al., 2006). As previously mentioned, biological tissue has both conducting and isolating properties, where the intra-and extracellular fluid conducts current, whilst the lipophilic cell membrane functions as an insulator. These properties are far from homogenous in soft tissue where cells vary in function and size. Approximately 80% of the cells in the liver are parenchymal hepatocytes responsible for secretory, endocrine and metabolic functions (Yang, 2021). The rest of the cell types in the liver are sinusoidal cells

including Kupffer cells and endothelial cells which contribute to the inhomogeneity of the organ. Kupffer cells constitutes approximately 15% of liver cells and are specialized macrophages within the liver functioning primarily as immune cells protecting the liver from bacterial infections (Gordillo et al., 2015). Kupffer cells are attached to endothelial cells which make up the walls of the blood vessels. Structure of the different cell types is illustrated in Figure 2.8. The different cells in the liver undergo a range of pathophysiological changes during ischemia which can influence the electrical properties of the liver tissue.
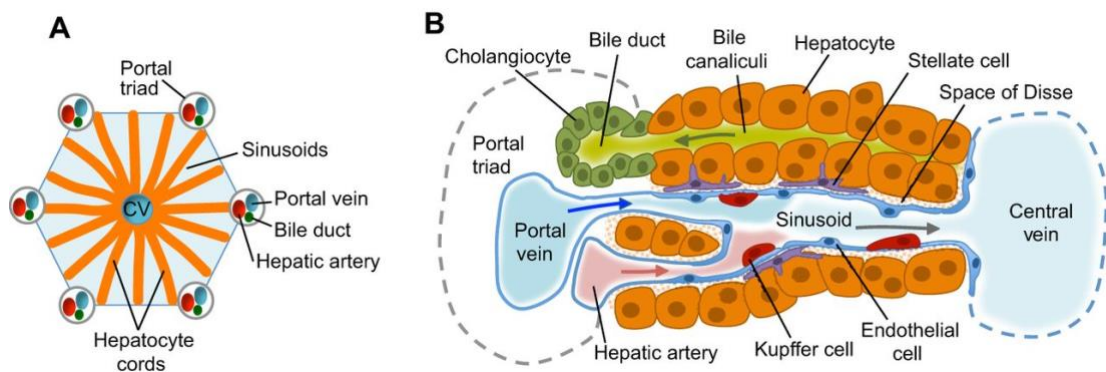
Figure 2.8: *Liver structure and cell types. (a) Anatomy of parenchymal liver lobules, each composed of a central vein and hepatic chords radiating out to portal triads consisting of portal vein, bile duct and hepatic artery. (b) Cell structure in the liver cell plate in parenchymal liver lobule (Gordillo et al., 2015).*

2.2.2 Ischemia-Reperfusion Injury in the Liver

There are two phases which contribute to the extent of IRI in organs: the magnitude and duration of deficient blood supply to the tissue and the restoration of blood supply to hypoxic tissue. Quick restoration of sufficient blood flow in the organ is therefore important to limit cell dysfunction, cell death and cell injury (Kalogeris, Baines, Krenz, & Korthuis, 2012).

Both warm ischemia taking place in-vivo and cold ischemia taking place intraoperatively or more commonly for organ preservation, are associated with initiating a cascade of complex immunological responses upon reperfusion. Initially in-vivo, warm ischemia leads to gradual cellular swelling as a result of the sodium-potassium

membrane pump malfunctioning. The interruption in blood flow is accompanied by lack of oxygen and nutrients as the cell metabolism turns anaerobic (S. Grimnes & Martinsen, 2017). During temperature drop in a cold storage cell, tissue metabolism is slowed which delays irreversible tissue damage prior to reperfusion. Cold storage organ preservation for human donor grafts is generally set to 5 - 8 hours in Norway, however SCS in this experiment was set to 18 – 20 hours to establish a marginalised liver model with overall hepatic injury. In contrast to warm ischemia where parenchymal hepatocellular injury dominates, the endothelial cells are particularly susceptible to apoptosis and coagulative necrosis after prolonged cold ischemia which consequently correlates with low liver viability upon reperfusion (Klune & Tsung, 2010). Furthermore, increased cold storage time correlates with increased activation of Kupffer cells upon reperfusion. The Kupffer cells produces reactive oxygen-species (ROS) and increases cytokine production, an inflammatory pathway which presents further pathogenic injuries upon reperfusion (Klune & Tsung, 2010). Although reperfusion is necessary to return to aerobic cellular metabolism, excess of oxidative stress on hypoxic tissue can cause cell injury (Kalogeris et al., 2012). Combined with activation of a cascade of inflammatory immune responses, locally and systemically, reperfusion itself can introduce or exacerbate IRI.

The purpose of NMP is to limit IRI through maintaining cell metabolism at physiological temperature, avoid accumulation of metabolic by-products, reduce time of hypoxia caused by warm ischemia and/or organ explantation and avoid depletion of cellular energy reserves (Zhai, Petrowsky, Hong, Busuttil, & Kupiec-Weglinski, 2013). Observation of the organ upon reperfusion is therefore of great value for surgeons in observing indications of IRI presented in an organ.

2.2.3 Electrical Properties of Ischemic Liver Tissue

If blood flow is interrupted in-vivo, tissue oxygenation is compromised which causes anaerobic metabolism to occur. Warm ischemia leads to cellular swelling through osmosis which narrows the extracellular current path through the tissue which corresponds with increased tissue impedance below approximately 10 kHz due to low cell membrane permittivity at low frequency AC signals (S. Grimnes & Martinsen,

2017). Furthermore, an increase in resistivity in ischemic tissue can be caused by the absence of blood or open blood vessels (if the blood leaks out, or the blood vessels are mechanically closed), as blood behaves as an electrical conductor (Miklavcic et al., 2006).

When tissue is excised from a specimen, over time gradual development of necrosis will lead to a point of irreversible injury and eventually organ malfunction and death. After cell death the cell membrane loses the ability to uphold ionic gradients and with it its insulating properties, causing a decrease in resistivity (Geddes & Baker, 1967). Furthermore, the electrical parameters of tissue are temperature dependent where increasing temperature leads to increased conductivity (Foster & Schwan, 1989).

Although not extensively researched, there are some reports related to the use of bioimpedance to detect ischemic liver tissue in animal models. Haemmerich et al. (2002) measured the resistivity in three porcine livers in-vivo and ex-vivo for 12 hours post explantation in the frequency range 10 Hz to 1 MHz. The measurements were conducted using a four-electrode plunge electrode and results were fitted into a Cole-Cole model from which the intra- and extracellular resistance and cell membrane capacitance were extrapolated, see results in Figure 2.9.
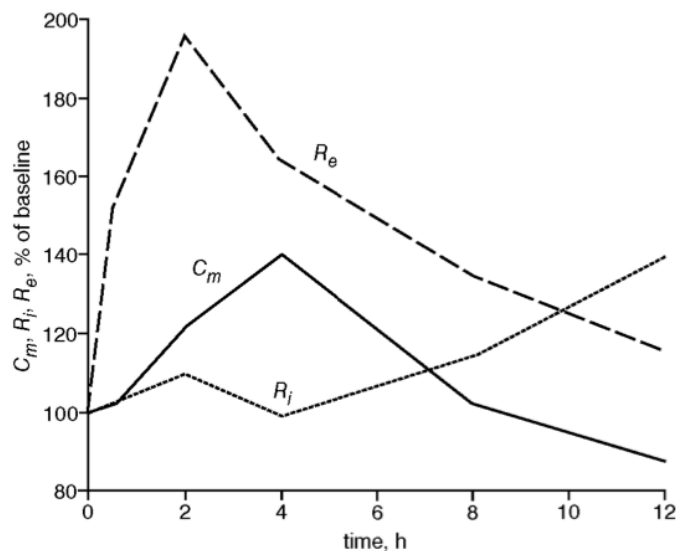
Figure 2.9: Changes in cell membrane capacitance (C_m), intracellular resistance (R_i) and extracellular resistance (R_e) during 12 hours after liver explantation, with h=0 being in-vivo (Haemmerich et al., 2002).

Similar results, supported by pathophysiological changes, were found by Al-Surkhi and Naser (2018) who measured Cole parameters of the liver post explantation in 10 rabbits. The measurements were conducted in periods up to 22 hours post excision in a frequency range between 1 kHz to 300 kHz. As for ischemia-reperfusion data there is not much to be found regarding liver, however Strand-Amundsen et al. (2018) found tissue state dependent changes in tanδ and φ to be of significance when investigating ischemia-reperfusion in porcine small intestine. Bioimpedance measurements using two-electrode trans-intestinal setup were performed in-vivo on 15 landrace pigs over warm ischemic periods between 1 - 16 hours and for 5 - 15 hours after reperfusion. Results showed a significant difference in tanδ between ischemic tissue and control tissue, as well as demonstrating that the frequency and amplitude of tanδ following reperfusion overlapped with or increased compared to ischemic tissue measurements, depending on ischemia time. The latter result indicating that reperfusion can introduce or exacerbate IRI as stated in section 2.2.2.

Chapter 3: Materials and Methods

This research project was approved by the Norwegian Animal Research Authority and follows the guidelines of the Animal Welfare Act.

3.1 Animals and Experimental Design

This study consisted of using 16 Norwegian Landrace pigs, where three pigs were used as a pilot to establish protocol for NMP and bioimpedance measurements. One experiment was terminated during machine perfusion due to a faulty temperature sensor, effectively preventing perfusion to continue. The statistical results are based on the remaining 12 pigs. The weight range of the pigs was 50 – 60 kg. The 12 pigs were divided into three groups: control, biliary injury and static cold storage (SCS):

3.1.1 Control Group

Four-hour bioimpedance measurements in-vivo followed by excision of the liver. The liver went directly onto machine perfusion after procurement.

3.1.2 Biliary Injury Group

Four-hour bioimpedance measurements in-vivo with partial warm ischemia through occlusion of the hepatic artery, with the intent of creating injury to the biliary tree prior to excision of the liver. The liver went directly onto machine perfusion after procurement.

3.1.3 Static Cold Storage (SCS) Group

Four-hour bioimpedance measurements in-vivo followed by excision and 18-20 hours static cold storage in order to create overall liver injury prior to machine perfusion.

The measurements in all groups were conducted hourly for a total of four hours before the pigs were sacrificed by lethal dose of potassium chloride (100 mmol) and hepatectomy took place. Measurements were initiated again immediately upon cold machine perfusion, followed by hourly measurements until the end of normothermic perfusion. The liver was perfused for six hours in total; one hour of cold perfusion with Belzer UW® solution, followed by one hour blood perfusion gradually warming up to normothermic temperature, and finally four hours of normothermic perfusion.
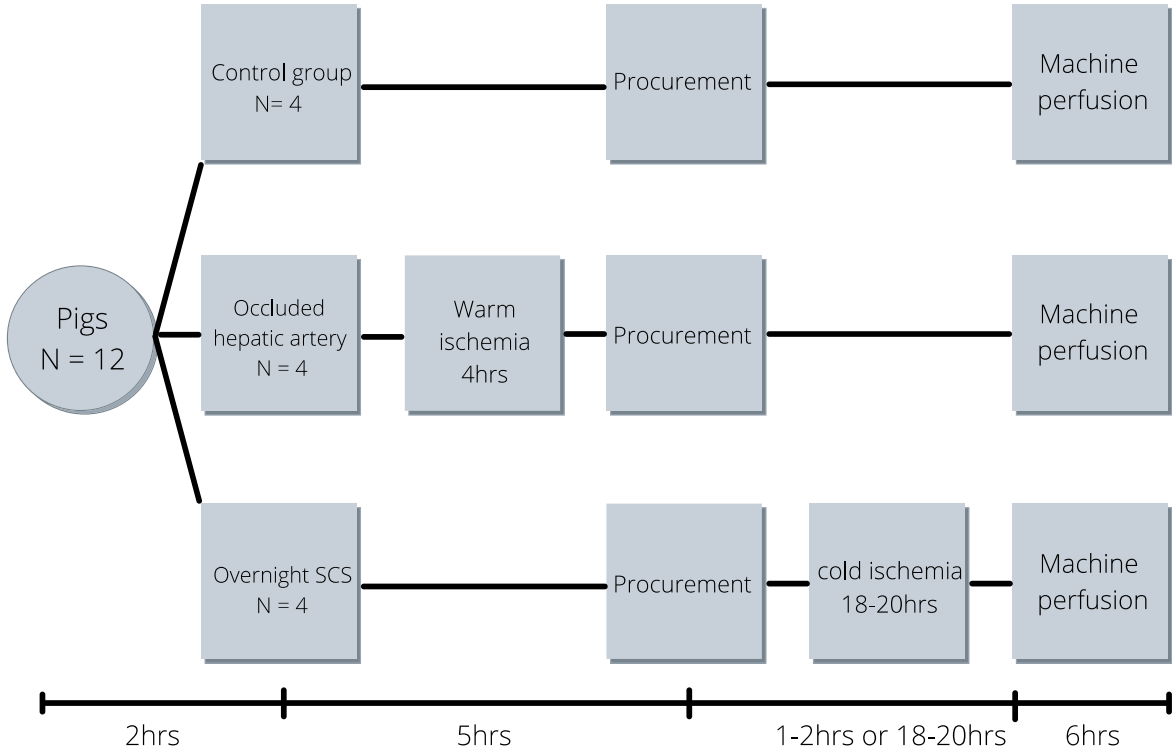
Figure 3.1: Overview of study protocol and timeline of each experiment.

Measurement Intervals	Comment
In-vivo 15min	Measurements start 15 minutes into the four hours in-vivo phase. Biliary injury group: 15 minutes after occlusion of hepatic artery.
In-vivo 1hr15m	
In-vivo 2hrs15min	
In-vivo 3hrs15min	
Reperfusion 15min	15 minutes after start of hypothermic perfusion with Belzer UW® solution.
Reperfusion 1hr15min	15 minutes after start of blood perfusion with gradual temperature rise to normothermic temperature.
Reperfusion 2hrs15min	15 minutes after blood perfusion at normothermic temperature.
Reperfusion 3hrs15min	
Reperfusion 4hrs15min	
Reperfusion 5hrs15min	

Table 3.1: *Protocol for measurement intervals. Time of measurement $\pm$10 minutes.*

3.2 Anaesthesia and Monitoring

The anaesthesia and analgesia protocol for the pig animal model was established in 2005 at Oslo University Hospital, and the research group has vast experience in regards of the protocol and keeping animal welfare as the highest priority throughout the experiments.

The pigs were transported to the hospital at least two days prior to the experiment to assure low stress level and good acclimatisation in the animal housing facilities. The welfare of the animal was monitored by trained personnel, and the pigs had free access to water and were fed until the night prior to the experiments.

On the day of the experiment the pigs were given an intramuscular injection consisting of ketamine (40 mg/kg), atropine (0.05 mg/kg) and droperidole (0.65 mg/kg). Prior to transportation an ear vein catheter was inserted, and the pigs were sedated with pentobarbital sodium (25 - 50 mg) and transported to an operating room. Additional pentobarbital sodium was administered if necessary.

On the operating table the pigs were placed in a supine position and hooked up to an intravenous infusion pump of morphine (1 mg/kg/hr), with a bolus of morphine or propofol administered if needed. After anaesthesia was obtained, a tracheotomy was performed to allow for the insertion of an endotracheal tube to allow mechanical ventilation. Analgesia was initiated through isoflurane (1.0 - 1.5 %) in-air oxygen and given continuously for the duration of the surgical procedure. The ventilator settings were adjusted throughout the experiments to maintain normal

pH (7.40), SaO2 > 94% and PaO2 > 8. The jugular vein was cannulated in order to monitor central venous pressure, allow for Ringer acetate and morphine infusion, and allow for intermittent blood sampling.

In addition to monitoring the respiratory parameters, an arterial pressure transducer was inserted into the right carotid artery to ensure mean arterial pressure was kept above 50 mmHg. The body temperature was measured through insertion of a urinary catheter via cystostomy.

3.3 Surgery

Surgery was conducted in operating room under sterile conditions. The liver was visualised through a median laparotomy, see Figure 3.2. Measurements were conducted for four hours until the liver was excised. For the biliary injury group, the hepatic artery was clamped after laparotomy to create warm ischemia in the biliary structures. Microdialysis catheters (M Dialysis AB, ISCUSflex Microdialysis Analyzer, Stockholm, Sweden, www.mdialysis.com) and pCO2 catheters (Sensocure AS, IschAlert^{TM}, Skoppum, Norway, www.sensocure.no) were placed in the liver tissue, the common bile duct and hilar plate, respectively. The right lateral lobe and right medial lobe were used for hourly trans-lobe bioimpedance measurements.

At the end of the in-vivo observations, 20,000 units of Heparin were administered, and 2.5 - 3 litres of blood were drained into collection bags, to be used for machine perfusion. An intravenous injection of pentobarbital sodium (500 mg) and potassium chloride (KCL) (40 mmol) were used for euthanasia prior to liver explantation, see excised liver in Figure 3.2.
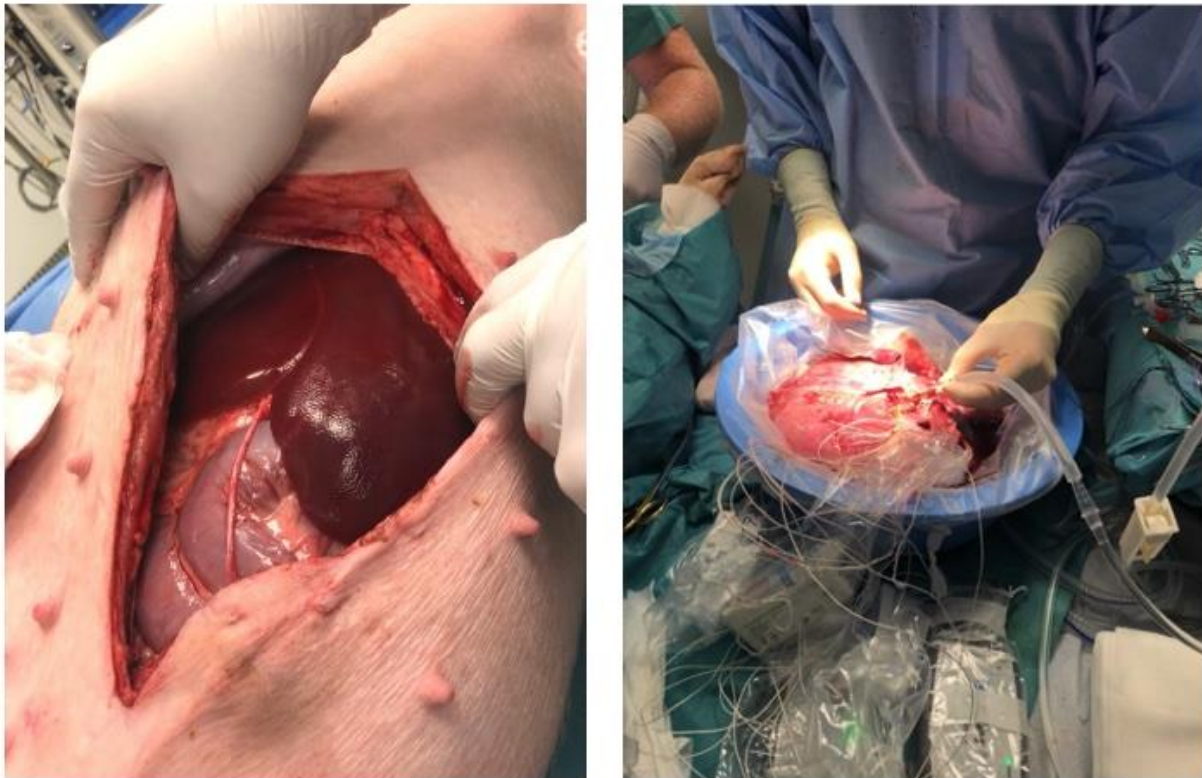
Figure 3.2: *Left: visualisation of the liver through median laparotomy. Right: excised liver flushed with organ preservation fluid prior to being connected to perfusion machine.*

3.4 Machine Perfusion

Oslo University Hospital has recently purchased a Liver Assist perfusion machine (Organ Assist Products B.V, Liver Assist, Groningen, The Netherlands, www.organ-assist.nl) to use the DHOPE-COR-NMP protocol for liver grafts. The explanted SCS livers were connected to the perfusion machine after 18-20 hours of cold storage time. The control group and biliary injury group also endured cold storage for a short transportation stage of approximately 15-30 minutes.

The Liver Assist perfusion machine consists of a hepatic artery pump unit and a portal vein pump unit, both equipped with pressure controlled rotary pumps allowing for pulsatile and continuous perfusion, respectively. The units are connected to hollow fibre oxygenators for dual oxygen reperfusion (Rijn et al., 2016), see Figure 3.3. A thermo unit controlled the perfusion temperature allowing transition from hypothermic to normothermic conditions

throughout the DHOPE-COR-NMP reperfusion protocol. After the circuit was primed, the livers were placed in an organ chamber and connected to a venous and arterial line. A chamber lid ensured a humid environment between hourly bioimpedance measurements. The bile duct was cannulated to allow for bile collection. The experiments ended after four hours of reperfusion at normothermic temperature. The perfusion machine was stopped, and the porcine livers were discarded of.
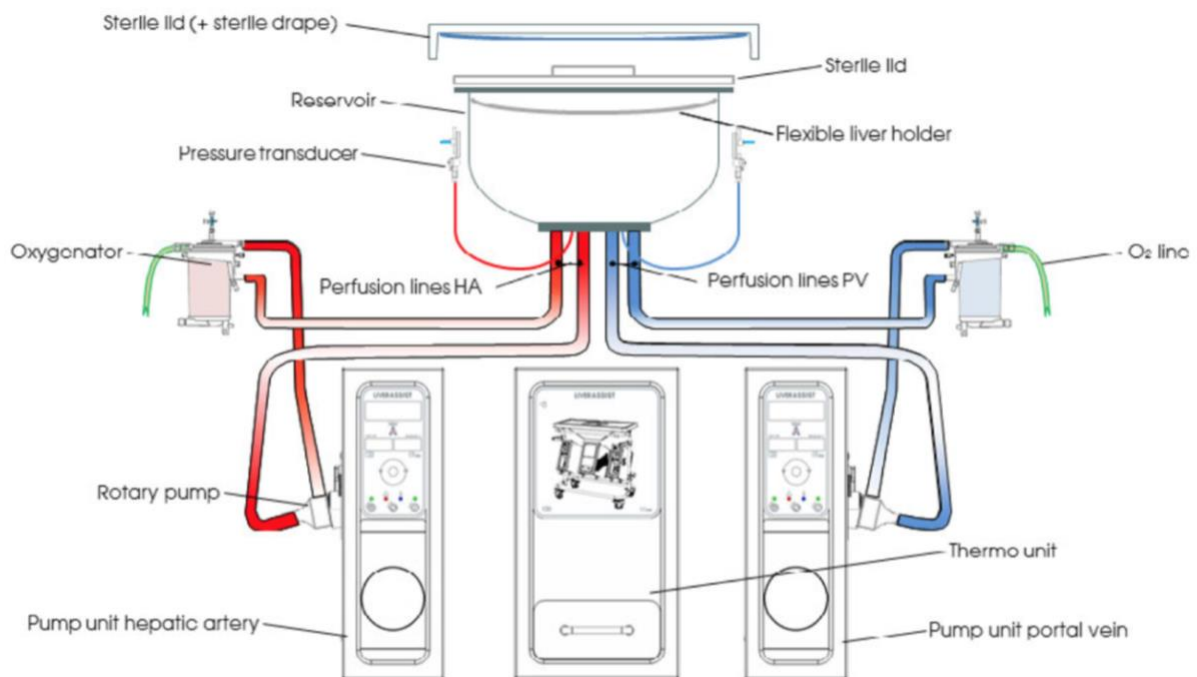
Figure 3.3: *Schematic drawing of dual normothermic machine perfusion (Rijn et al., 2016).*
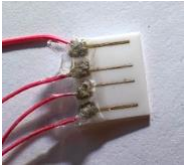
3.5 Bioimpedance Measurements

Bioimpedance measurements were executed by the Solartron 1260A Impedance/Gain-Phase Analyzer (Solartron Analytical, Leicester, England, www.ameteksi.com). The measurements were conducted with an AC amplitude set to 100 mV over a frequency range from 100 Hz to 1 MHz. The real-time data throughput was enabled by the Zplot® measurement software (Scribner Associates Inc. ZPlot® for Windows, North Carolina, USA, www.scribner.com) and transferred to SPSS® Statistics software (IBM Corp. Released 2020. IBM SPSS Statistics for

MacBook, New York, USA, www.ibm.com) and GraphPad Prism (GraphPad Software, California, USA, www.graphpad.com) for further analysis.

3.5.1 Methodological Considerations for Electrode Design

There were several methodological considerations to run through prior to and during the pilot experiments to select an electrode setup that could be stable in measurements of the electrical properties of the liver. All electrode systems were initially tested in saline solution (0.9%) to measure inductance and EPI contributions. The four remaining electrode systems of interest (two-electrode Ag/AgCl setup, two-electrode carbon setup, four-electrode gold row setup and two-electrode sintered Ag/AgCl setup) were tested in experimental pilots on liver tissue to investigate sensitivity to pressure variations and external noise contributions in-vivo (see summary in Table 3.2).

Electrode setup	Site of measurement		Saline Solution	Liver in-vivo
Two-electrode setup with Ag/AgCl electrocardiography electrodes	Transverse liver lobe		Very low EPI < 1 kHz Impedance < 20 Ω	Low sensitivity to pressure variation Low noise Reproducible results
Two-electrode setup with carbon disc electrodes	Transverse liver lobe		High EPI < 1 kHz Impedance < 100 Ω between 1 kHz and 1 MHz	High sensitivity to pressure variation Unreliable measurements
Four-electrode setup with gold row electrodes	On top of liver lobe		Insignificant EPI Impedance < 20 Ω	High sensitivity to pressure variation Unstable setup Unreliable measurements
Two-electrode setup with sintered Ag/AgCl electrodes	Transverse gall duct		Very high EPI < 100 kHz Impedance < 100 Ω between 100 kHz and 1 MHz	Unreliable measurements

Table 3.2: *Test of electrodes in NaCl (0.9%) and in-vivo on porcine liver during pilot experiments.*

Initially we were interested in measuring bioimpedance on the gall duct, as well as on the liver lobe, to investigate changes in electrical parameters directly linked to biliary structures. The two-electrode sintered Ag/AgCl electrodes were tested on the gall duct in-vivo, however it proved challenging to measure with the setup due to the thin duct wall and measurements taking place in-situ with bile present, behaving as an interfering dielectric component when investigating the small signals of the thin gall duct wall. Due to gall duct biopsies being sent to pathology, we did not have enough remaining gall duct tissue to excise samples to measure ex-vivo. Combined with time restraint, investigation of the bile duct was rejected, and the main focus was set to establishing the optimal electrode system for liver lobe measurements.

In Figure 3.4 we show |Z| and φ for the electrode systems tested in saline solution at room temperature. We observe that the impedance and EPI measured with the Ag/AgCl and gold electrode systems are the lowest of the chosen setups. This is probably because of the large area of the Ag/AgCl electrodes combined with the surface properties of this material, and due to the four-electrode setup of the gold electrode systems, which measures transfer impedance. Measurements in saline solution with the two-electrode carbon setup demonstrated high EPI contributions at frequencies below 1 kHz. The sintered Ag/AgCl electrodes had very high EPI dominating up to 100 kHz. Note that the sintered Ag/AgCl electrodes were tested transversely on the gall duct in-vivo. All the electrode setups showed inductive stray properties at high frequencies when measuring on low impedances, resulting in a positive phase. The inductance is more evident when measuring in system with small loads such as the saline solution and can be subtracted from the measured results to correct the data.
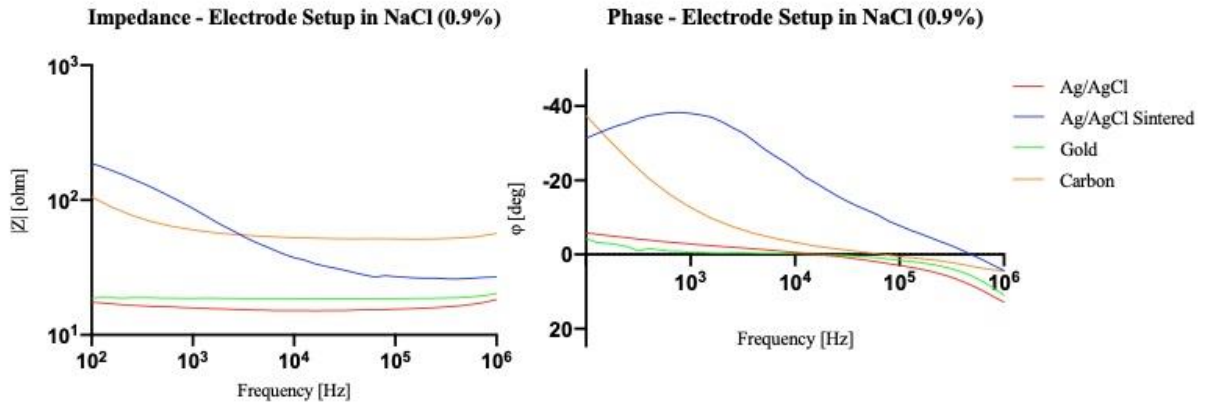
Figure 3.4: *Electrode designs tested in saline solution at room temperature and presented as |Z| and φ vs. frequency.*

In Figure 3.5 we show the electrode systems tested in the first hour of in-vivo measurements on porcine liver. As expected, the Ag/AgCl electrodes exhibited the lowest sensitivity to pressure variation as well as the lowest noise contribution from external factors out of all the electrode systems. An example of such an external factor being respiration movements during in-vivo measurements. We measured a higher contact impedance with the carbon electrodes than with the Ag/AgCl electrodes, and the probable cause was the relatively smaller area of the carbon electrodes. Furthermore, stable fixation on the lobe proved challenging due to high sensitivity of the setup for pressure changes, movement and vibration, resulting in measurement artifacts. The gold electrode system measured low transfer impedance in the liver (left) and a reduced amplitude of φ with a vertical shift between 100 kHz and 1 MHz due to the stray inductance of the electrode setup and wires (right). Although the properties of the gold electrode were of interest, the setup was not optimal as the sensitivity to pressure variation was high and we did not have an electrode holder ensuring exact pressure for each measurement.
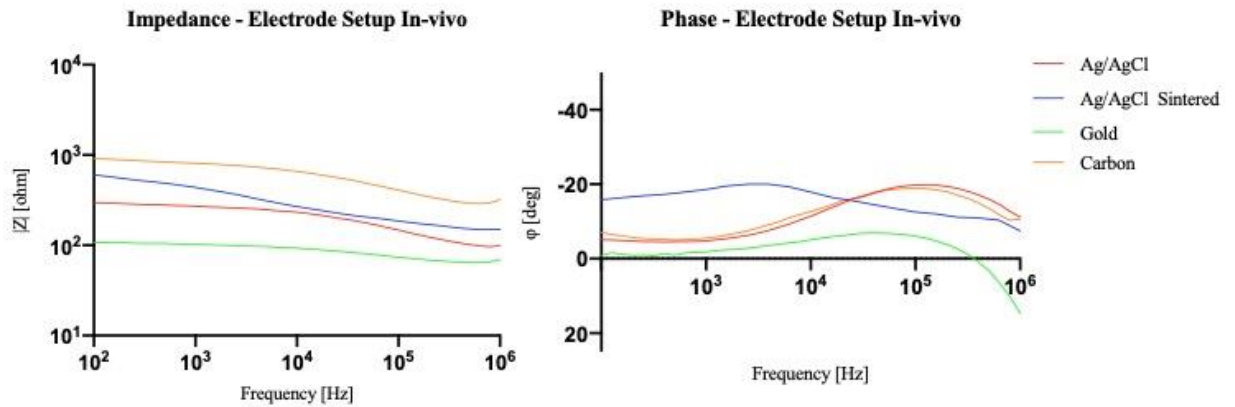
Figure 3.5: *Electrode designs tested in-vivo on porcine liver and presented as |Z| and*
φ vs. frequency.

The final decision landed on the two-electrode system consisting of a pair of Ag/AgCl electrocardiography electrodes (Cardiolex Medical AB, Quickels filter electrodes, Solna, Sweden, www.cardiolex.com). The Ag/AgCl electrodes demonstrated low sensitivity to pressure variation and had low noise contribution, allowing for reproducible and reliable measurements. For every experiment, the electrodes were submerged in saline solution (0.9%) prior to measurements to make sure the electrode/electrolyte interface was saturated in liquid and would not cause a drift in the measurements. The electrodes were attached to each their grabber clip, connected to the input and output banana plugs from the Solartron interface. The grabber clips were connected together, allowing for an approximately even transverse pressure from the electrode surfaces on the tissue surface (see Figure 3.6). Each measurement was conducted approximately three centimetres down from the edge of the right lateral lobe or right medial lobe, whichever was of the optimal thickness in order to obtain a consistent pressure between electrodes and tissue. During measurements the electrode holder rested on a dry cloth to prevent contact with surrounding dielectrics and limit motion disturbance from respiration.

Figure 3.6*: Left: two-electrode system with Ag/AgCl electrodes. Right: in-vivo measurements on liver lobe using Ag/AgCl electrodes.*

3.5.2 Impedance/Gain-Phase Analyser

The Solartron 1260A uses a single-sine method, where frequency measurements up to 300 Hz are measured by an analogue to digital converter (ADC). At frequencies above 65.5 kHz an analogue phase-locked loop generates an internal high-frequency reference signal and a high frequency signal to the sample measured. The internal reference signal is slightly offset from the output signal. The input signal is combined with the reference signal to yield a frequency sum and difference, where the frequency sum is filtered out. Consequently, we are left with a low-frequency waveform which is then analysed by the ADC. This process is called heterodyning, and a digital version of the process occurs for the midrange frequencies (300 Hz – 65.5 kHz) in order for the resulting low-frequency waveform to be analysed by the ADC (S. Grimnes & Martinsen, 2017). The Solartron 1250A was connected to a preamplifier, 1294 Impedance Interface (Solartron Analytical, Leicester, England, www.ameteksi.com), acting as a dielectric interface necessary to comply with the IEC 61010-1 safety regulations for use of connection of electrical equipment to live subjects (S. Grimnes & Martinsen, 2017). The interface uses driven shields to avoid leakage current and has high input impedance to ensure that the device will not draw any current from the subject.

3.5.3 Experimental Bioimpedance Protocol

Prior to tissue measurements the Ag/AgCl electrodes were submerged in a tub with saline solution (0.9%) to avoid drift, as previously stated. The input/output banana plugs of the Solartron 1294 Impedance Interface were configured to a two-electrode setup and connected to an impedance test load to validate that the system provided accurate measurements. When attached to the electrode system, we measured the short impedance and the air between the electrodes' impedance (revealing the electric properties of the setup and stray effects influencing the measurements).

Pathophysiological changes in ischemic tissue are fairly slow, thus hourly measurement intervals were deemed fitting to observe changes in the electrical properties of the liver. Measurements began approximately 15 minutes after the liver had been made available by the surgeon through medial laparotomy (see measurement intervals in Table 3.1). For the partial warm ischemia group, the first measurement was taken approximately 15 minutes after occlusion of the hepatic artery. Prior to each measurement the intended spot for measurement on the liver lobe was carefully wiped to remove liquid drops acting as dielectric components potentially interfering with our measurements. After four hours of in-vivo measurements hepatectomy was performed and measurements were resumed when the liver was perfused with cold Belzer UW® solution on the perfusion machine. Measurements were conducted every hour until the end of NMP.
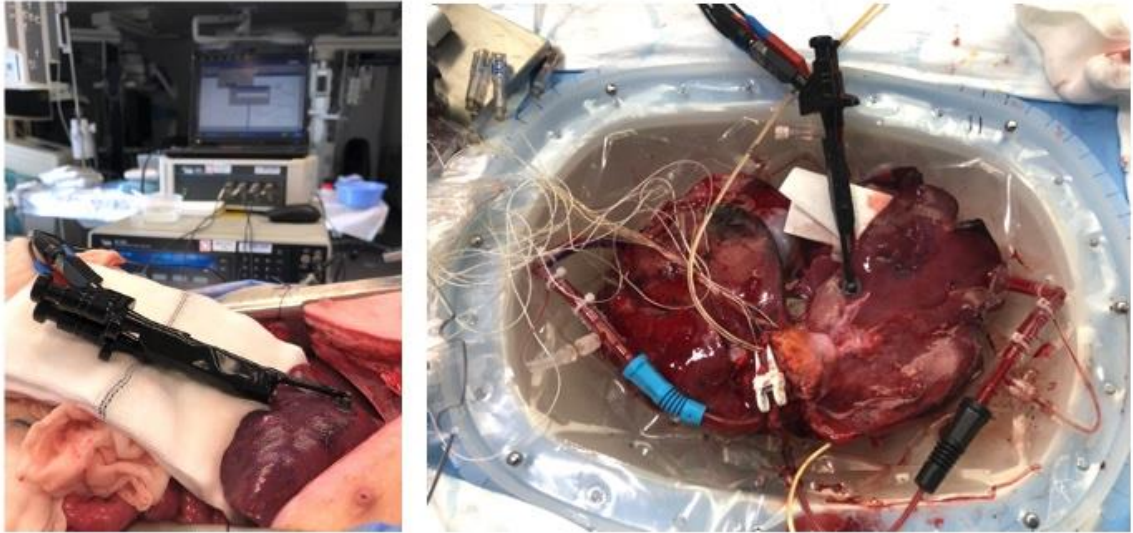
Figure 3.7: *Left: in-vivo measurements with Solartron 1260A and Solartron 1294 Impedance Interface in the background. Right: reperfusion measurement on the perfusion machine.*

3.6 Data Evaluation

The measured data was collected using ZView® software and was converted from ".z" files to ".txt" files and transferred to MacBook for further organisation, calculation and statistical analysis. Based on the research of Strand-Amundsen et al. (2018), we were particularly interested in investigating ischemia-reperfusion changes in the ratio parameters; φ and $\tan\delta$, as well as looking at $|Z|$ to assess the tissue state. $|Z|$ is dependent on the distance between the electrodes in the trans-lobe measurements, whilst φ and $\tan\delta$ look at the relationship between the imaginary and real components of impedance and are less dependent on the thickness of the liver lobe.

3.6.1 Statistical Analysis

The data is visualized as mean values with standard deviation (SD) and with 95% confidence interval (CI). Statistical Analysis was performed using IBM® SPSS® Statistics software and the graphing and statistics software GraphPad Prism. The null hypothesis to be rejected is that there is no difference between the means of the three groups. As n = 4 for each group and the measurements in each group were repeated

measurements over independent factors (frequency and time), we investigated statistical differences between the groups with two-way analysis of variance (ANOVA) and Tukey's multiple comparisons test. The two-way ANOVA test is a factorial analysis where the results are based on whether any of the two independent factors in our datasets, frequency and time, results in significant differences between groups (control, biliary injury and SCS) by observing how the mean of a quantitative variable ($|Z|$, φ, $\tan\delta$ or $\tan\delta m$) changes as a function of the levels of said factors. The ANOVA test tells us if there are significant findings across groups, but to find where the exact differences lie, we use a multiple comparison test which determines significant differences through pairwise comparison of means of the independent observations between groups.

Chapter 4: Results

The raw data obtained from the measurements consists of complex impedance, described by real and imaginary properties (as stated in Chapter 2 equation 2.2) in the frequency range of 100 Hz to 1 MHz. Figure 4.1 shows a Wessel plot with the typical liver dispersions measured with the Ag/AgCl setup. From the raw data we calculated |Z| as well as the ratio parameters φ and $\tan\delta$, as seen in Chapter 2, equation 2.3, 2.4 and 2.5 respectively. Depending on greater change being measured in the nominator or denominator in the ratio parameter equations, we amplify changes in the relationship between the imaginary and real components of impedance that cannot be observed through |Z| alone. Frequency is displayed on a base-10 logarithmic scale to amplify dissimilarities in the low frequency measurements.

Complex Resistivity in Liver Tissue
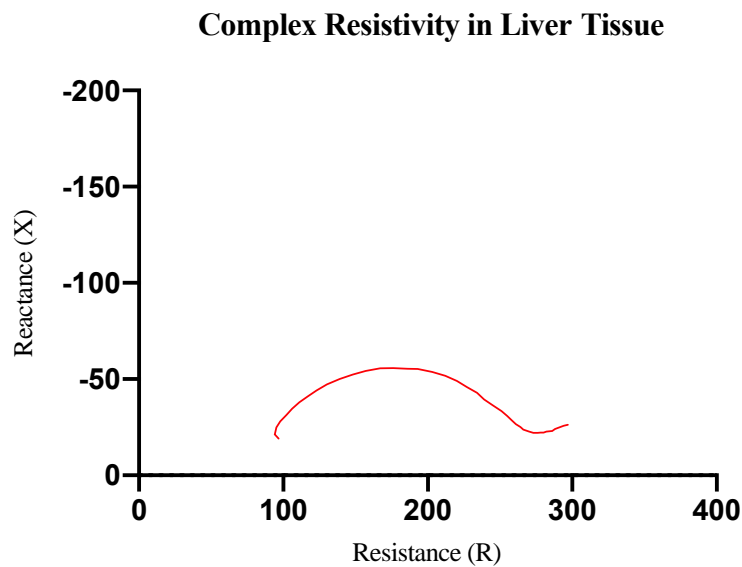
Figure 4.1: *Wessel plot of typical dispersion seen in-vivo on liver tissue measured with two-electrode Ag/AgCl setup. Measurement conducted over a frequency sweep starting to the left at 1 MHz down to 100 Hz to the right.*

A total of 12 porcine livers underwent investigation during in-vivo and DHOPE-COR-NMP perfusion protocol. Results from all groups (control, biliary injury and SCS) are represented as mean of each group at the same time-interval, where n = 4 pigs for each group.

4.1 Impedance Modulus

Figure 4.2 shows the overall trend of change in |Z| in all three groups throughout the experiments. The impedance modulus has a large increase in amplitude at the start of reperfusion in all groups. Throughout the next two hours of reperfusion, a steady decrease in amplitude of |Z| follows for all groups. Figure 4.2 does not display error for readability purposes.
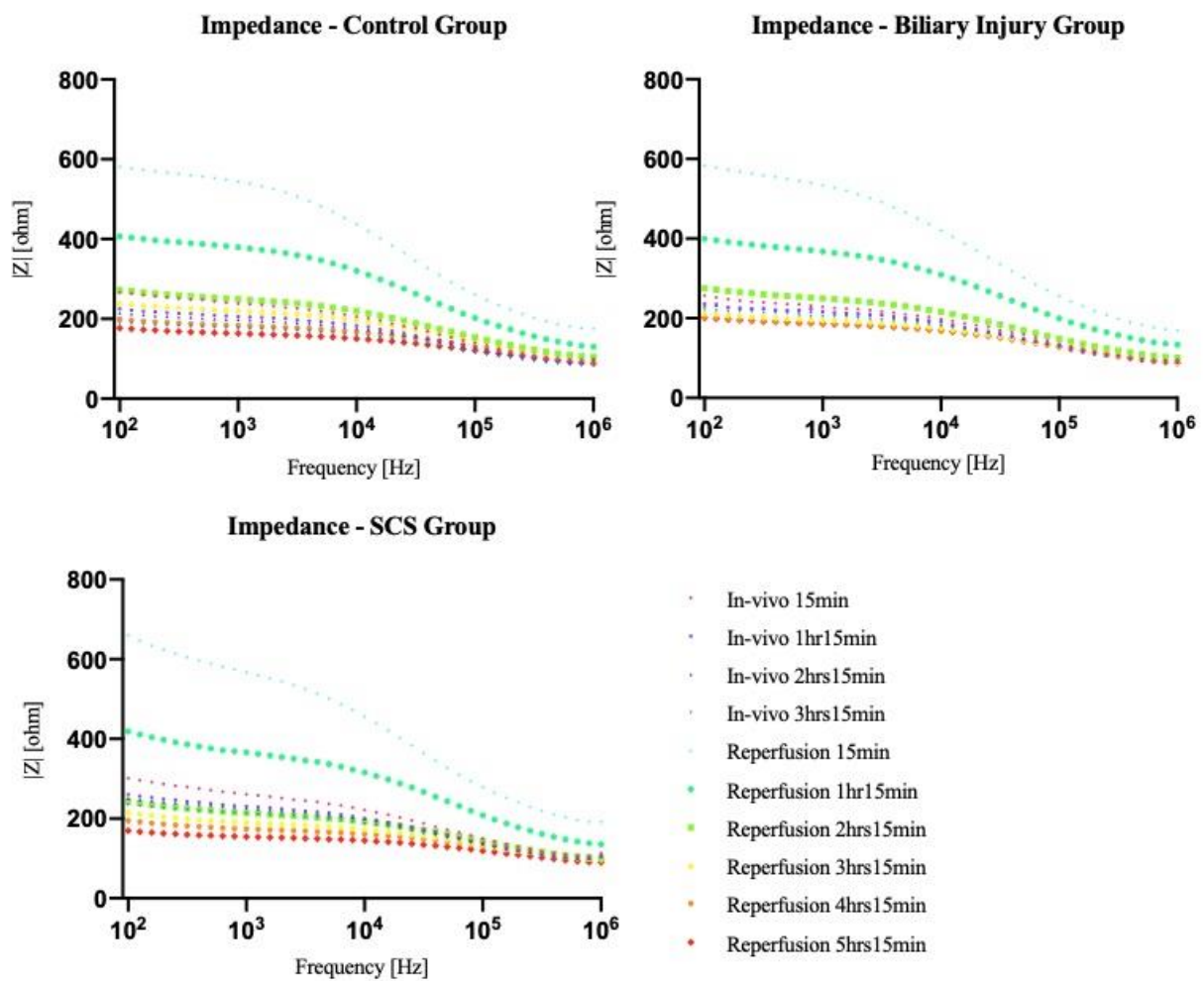
Figure 4.2: *Mean of |Z| vs. frequency throughout the experiments. Top left: control group (n = 4 pigs). Top right: biliary injury group (n = 4 pigs). Bottom: SCS group (n = 4 pigs).*

In Figure 4.3 we show the trend of |Z| at three selected time points: at the very start of in-vivo measurements (top left), after ischemia in the first 15 minutes of hypothermic reperfusion (top right) and at the end of NMP (bottom). The mean of each group is similar at each time of measurement; however, we see much larger SD values at low frequencies in "reperfusion 15min" (top right). Two-way ANOVA tests conducted with Tukey's multiple comparison test determined no significant differences in |Z| between the groups at any time interval throughout the experiments.
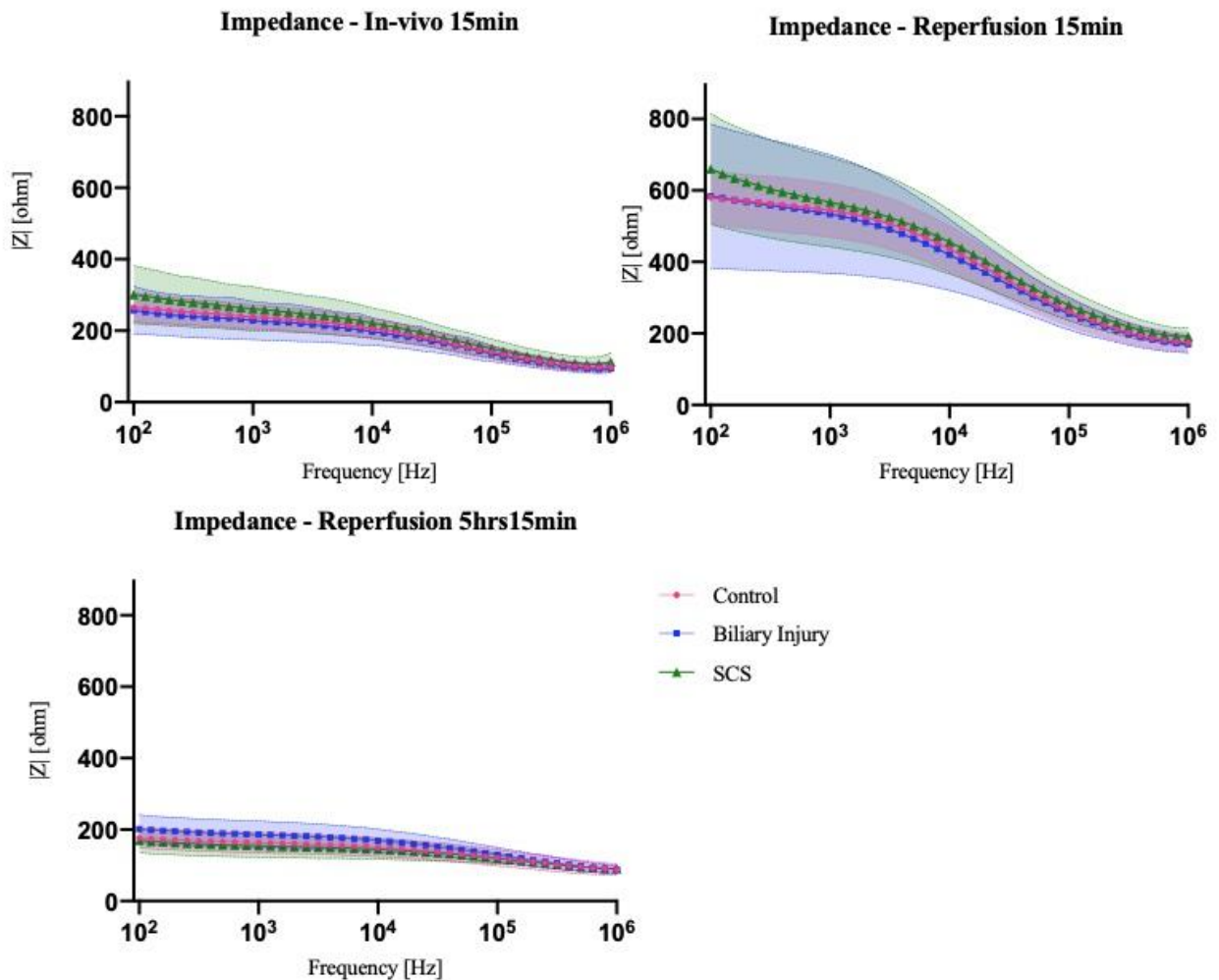
Figure 4.3: *Group comparison plots of the mean of |Z| with SD vs. frequency. N = 4 pigs for each group. Top left: start of in-vivo measurements. Top right: start of hypothermic reperfusion. Bottom: end of normothermic reperfusion.*

4.2 Phase

Figure 4.4 shows the trend in change of φ for each group separately throughout the experiment and are represented as mean of measurements at the same time-interval. Figure 4.4 does not display error for readability purposes. The three graphs demonstrate a similar trend where the amplitude of φ is increased for "reperfusion 15min" and "reperfusion 1hr15min". In the remaining measurements during NMP the amplitude of φ decrease below that of the amplitude in the in-vivo measurements. Additionally, we notice a phase-shift towards the right for all groups upon NMP.
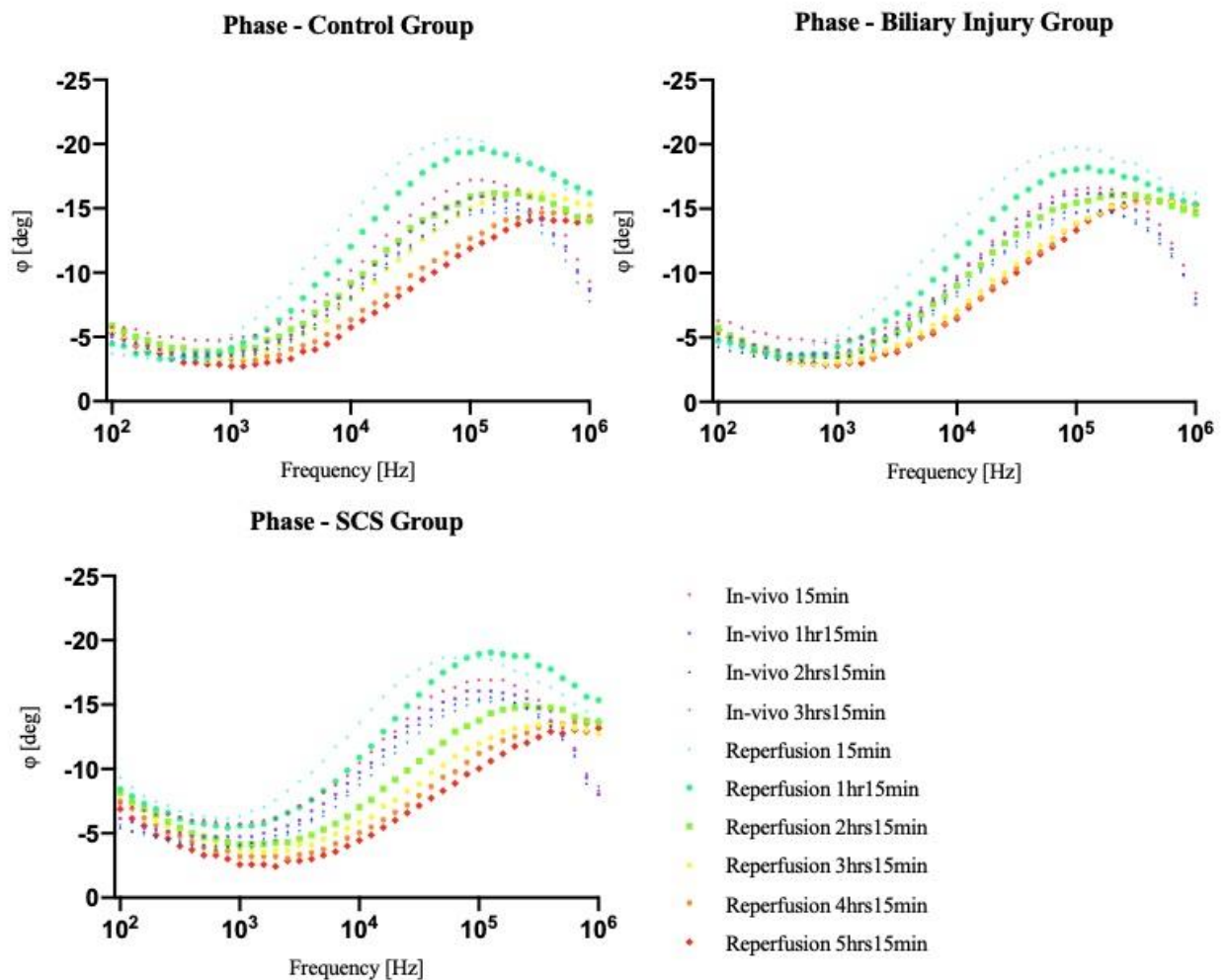
Figure 4.4: *Mean of φ vs. frequency throughout the experiments. Top left: control group (n = 4 pigs). Top right: biliary injury group (n = 4 pigs). Bottom: SCS group (n = 4 pigs).*

Figure 4.5 shows comparison plots of the groups (control, biliary injury and SCS) at three selected times of measurement, where φ of each group is represented as mean with SD. Looking at "reperfusion 15min" (top right), notice the SCS group displaying a steeper slope in φ between 100 Hz and 1 kHz compared to the two other groups. At the end of NMP (bottom) we see an overall lower amplitude of the φ with a broader error band at higher frequencies, especially for the SCS group.
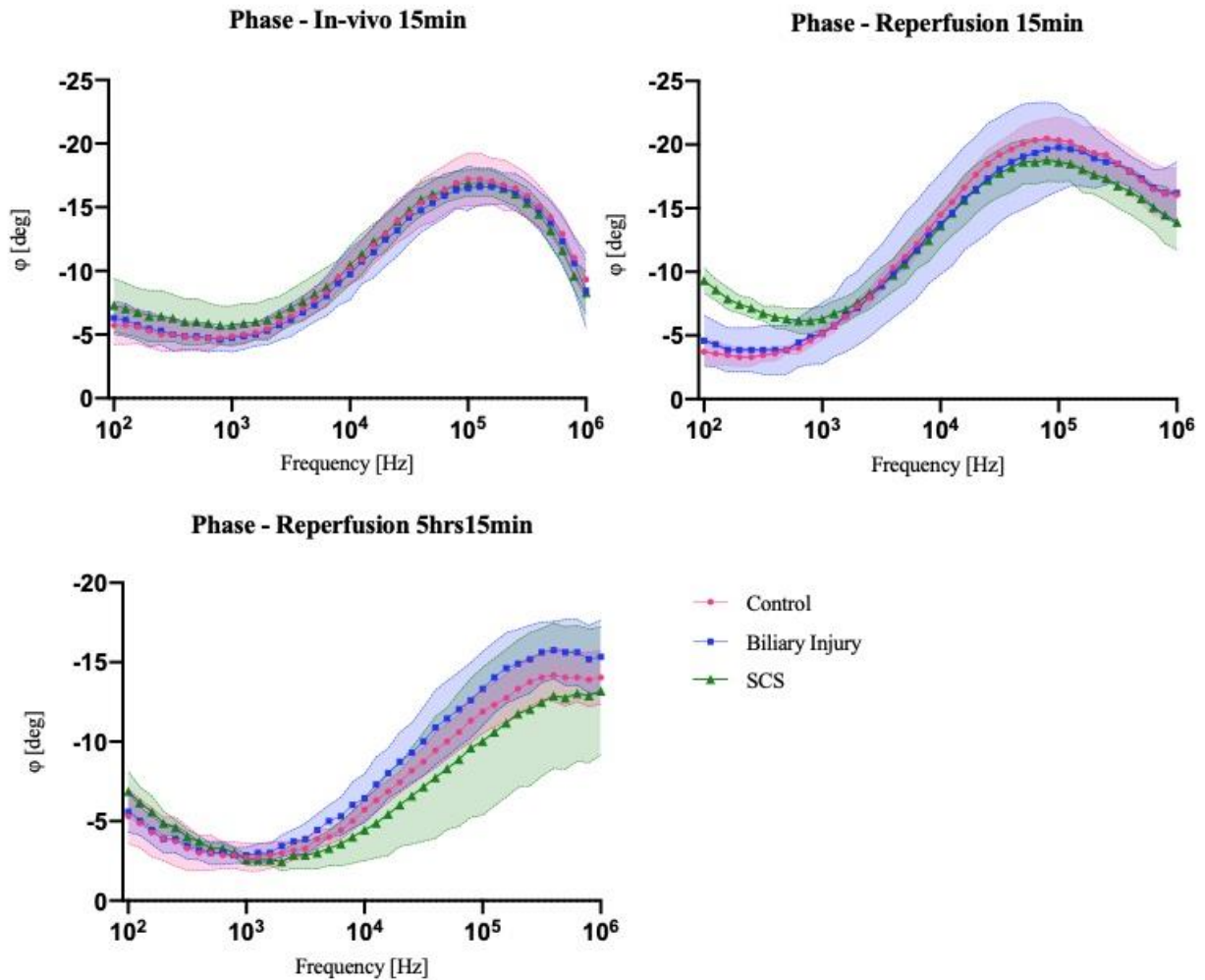
Figure 4.5: *Group comparison plots of the mean of φ with SD vs. frequency. N = 4 pigs for each group. Top left: start of experiment. Top right: start of hypothermic reperfusion. Bottom: end of normothermic reperfusion.*

Two-way ANOVA tests conducted with Tukey's multiple comparison test determined significant differences in φ between groups in "reperfusion 15min" and "reperfusion

1hr15min" shown in Table 4.1 and 4.2. No significant differences in φ between groups were found in any other time interval throughout the experiments.

| Frequency [Hz]	Compared Groups	Mean Diff.	95% CI of diff.	Adjusted P Value
1000000.000	Biliary Injury vs. SCS	-2.293	-3.987 to -0.599	* 0.022
794328.000	Biliary Injury vs. SCS	-1.170	-2.698 to -0742	* 0.011
630957.000	Biliary Injury vs. SCS	-1.576	-3.084 to -0.069	* 0.045
630.957	Control vs. SCS	2.150	0.353 to 3.946	* 0.031
501.187	Control vs. SCS	2.436	0.929 to 3.943	* 0.014
398.107	Control vs. SCS	2.866	0.910 to 4.822	* 0.018
	Biliary Injury vs. SCS	2.580	0.086 to 5.073	* 0.046
316.228	Control vs. SCS	3.296	1.789 to 4.803	** 0.006
251.189	Control vs. SCS	3.869	1.602 to 6.137	* 0.012
	Biliary Injury vs. SCS	3.296	1.029 to 5.563	* 0.018
199.526	Control vs. SCS	4.156	2.359 to 5.953	** 0.005
	Biliary Injury vs. SCS	3.583	0.753 to 6.413	* 0.027
158.489	Control vs. SCS	4.433	2.175 to 6.710	** 0.008
	Biliary Injury vs. SCS	4.013	1.425 to 6.600	* 0.015
125.892	Control vs. SCS	5.016	2.547 to 7.485	** 0.007
	Biliary Injury vs. SCS	4.299	1.448 to 7.151	* 0.016
100.000	Control vs. SCS	5.589	2.439 to 8.739	* 0.010
	Biliary Injury vs. SCS	4.729	1.153 to 8.306	* 0.024

Table 4.1: *Frequencies during "reperfusion 15min" where significant differences in φ are found between groups. * = P < 0.05 and ** = P < 0.01.*

Frequency [Hz]	Compared Groups	Mean Diff.	95% CI of diff.	Adjusted P Value
794.328	Control vs. SCS	1.720	0.026 to 3.414	* 0.048
	Biliary Injury vs. SCS	1.720	0.026 to 3.414	* 0.048
630.957	Control vs. SCS	2.150	0.353 to 3.946	* 0.031
	Biliary Injury vs. SCS	1.863	0.356 to 3.370	* 0.029
501.187	Control vs. SCS	2.293	0.600 to 3.987	* 0.022
	Biliary Injury vs. SCS	2.150	0.353 to 3.946	* 0.031
398.107	Control vs. SCS	2.436	0.929 to 3.943	* 0.014
	Biliary Injury vs. SCS	2.293	0.106 to 4.480	* 0.044
316.228	Control vs. SCS	2.866	1.888 to 3.844	** 0.002
	Biliary Injury vs. SCS	2.580	0.505 to 4.654	* 0.028
251.189	Control vs. SCS	3.296	2.149 to 4.443	** 0.003
	Biliary Injury vs. SCS	2.866	0.680 to 5.053	* 0.024
199.526	Control vs. SCS	3.153	2.461 to 3.844	*** 0.0007
	Biliary Injury vs. SCS	2.866	0.100 to 5.632	* 0.046
158.489	Control vs. SCS	3.583	2.436 to 4.730	** 0.002
	Biliary Injury vs. SCS	3.010	1.213 to 4.806	* 0.012
125.892	Control vs. SCS	3.583	2.436 to 4.730	** 0.003
	Biliary Injury vs. SCS	3.296	0.827 to 5.765	* 0.013
100.000	Control vs. SCS	4.013	2.630 to 5.396	** 0.003
	Biliary Injury vs. SCS	3.726	1.433 to 6.020	* 0.013

Table 4.2: *Frequencies during "reperfusion 1hr15min" where significant differences in φ are found between groups. * = P < 0.05, ** = P < 0.01 and *** = P < 0.001.*

4.3 Tanδ

Changes in tanδ over time are shown in Figure 4.6 with a graph plotted separately for each group, represented as mean of measurements at the same time-interval. Figure 4.6 does not display error for readability purposes. An overall increase in amplitude of tanδ through the duration of reperfusion is observed. Note the decreased amplitude of tanδ at "reperfusion 15min" in the SCS group (bottom) prior to the amplitude increasing further on in the reperfusion protocol.
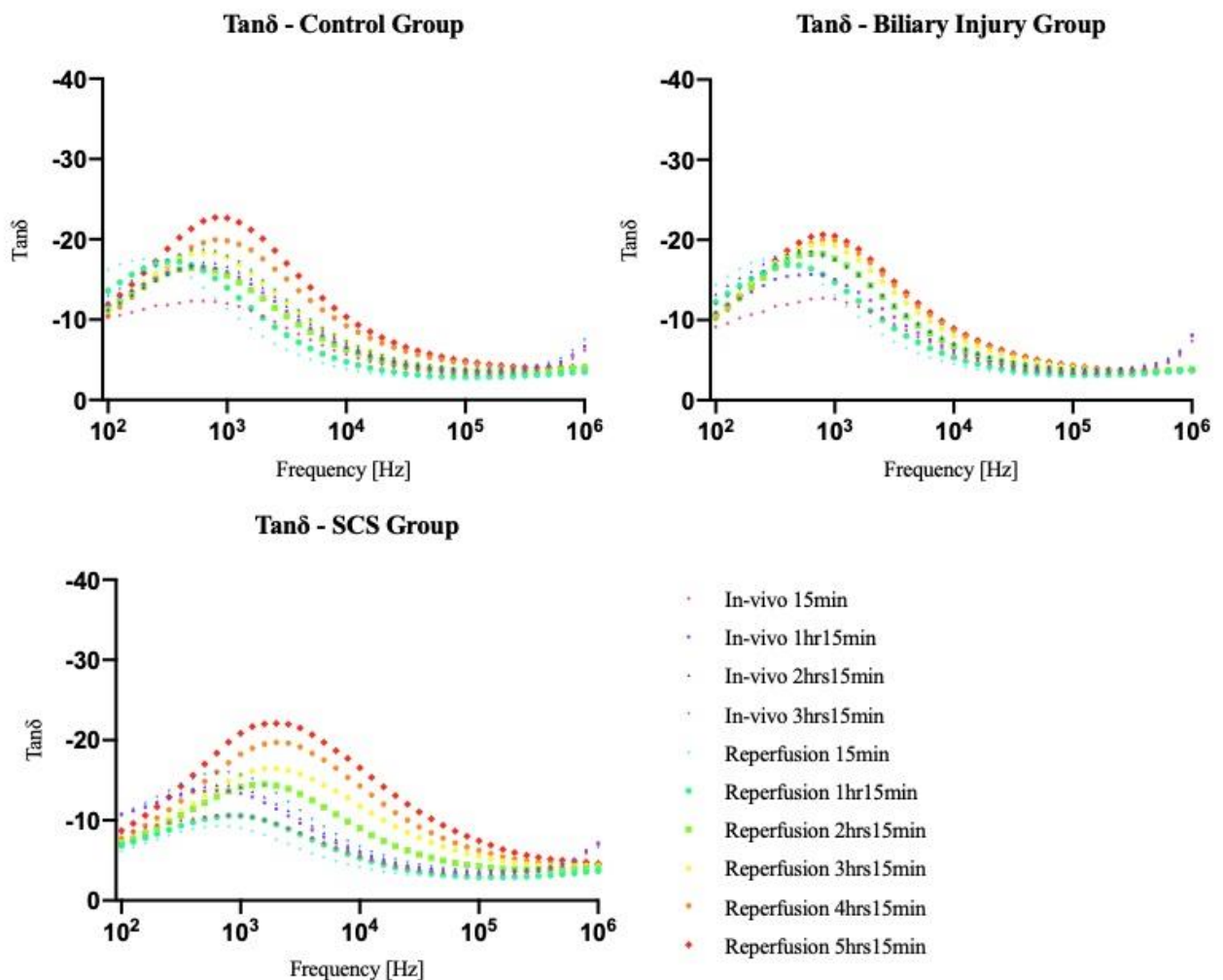
Figure 4.6: *Mean of tanδ vs. frequency throughout the experiments. Top left: control group (n = 4 pigs). Top right: biliary injury group (n = 4 pigs). Bottom: SCS group (n = 4 pigs).*

Figure 4.7 shows the comparison of tanδ between the groups at three selected time-intervals throughout the experiment, and are represented as the mean of each group with SD. In the "reperfusion 15min" time-interval (top right) we see a phase-shift to the left and an increase in amplitude of tanδ for the control group and biliary injury group. Note the small SD for SCS comparatively. At the end of NMP (bottom) a phase-shift to the right is observed for all groups as well as an increase in amplitude of tanδ. Compared to the control and biliary injury groups, the SCS group has the largest amplitude increase over the span of reperfusion.
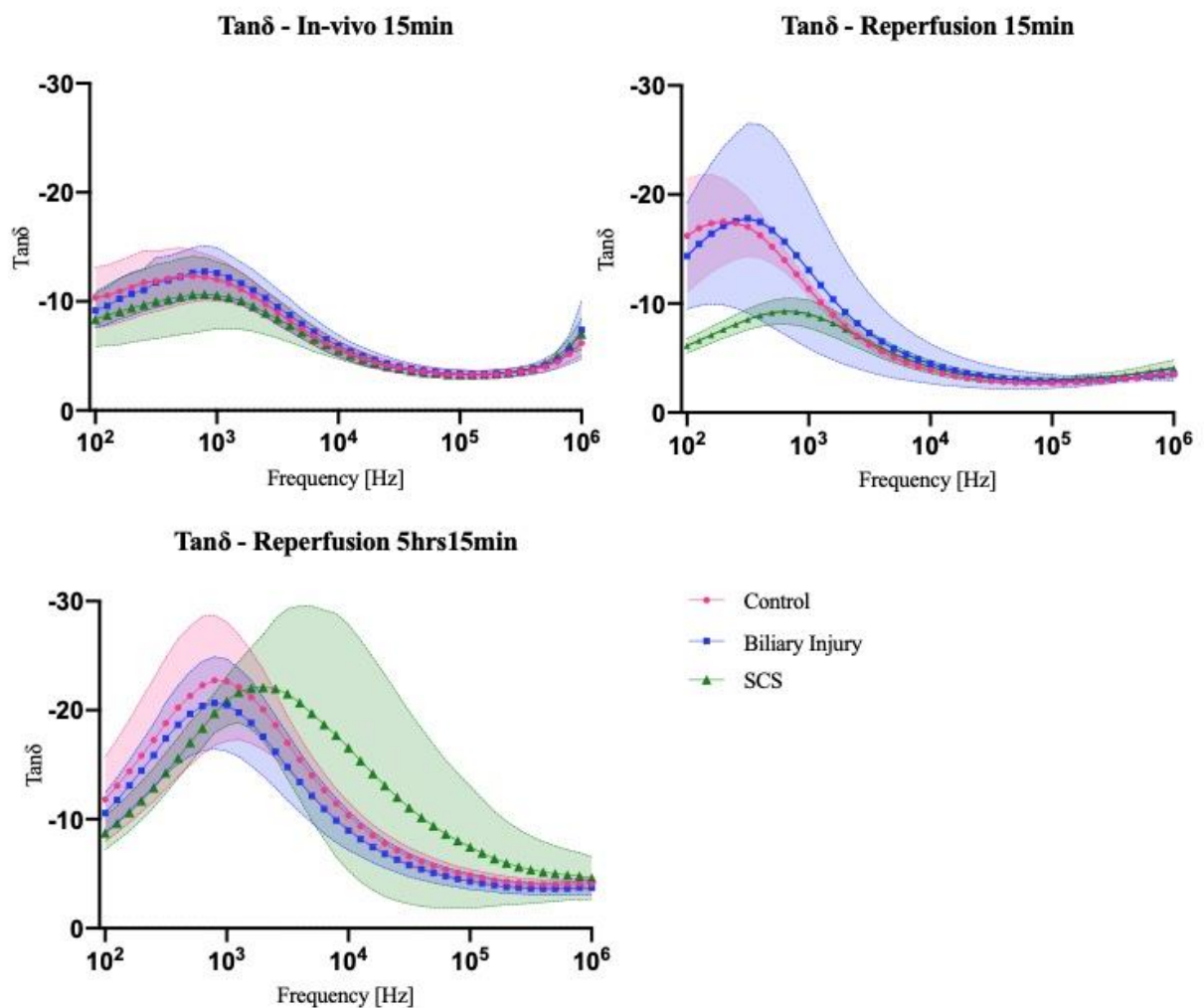
Figure 4.7: *Group comparison plots of the mean of tanδ with SD vs. frequency. N = 4 pigs for each group. Top left: start of experiment. Top right: start of hypothermic reperfusion. Bottom: end of normothermic reperfusion and end of machine perfusion.*

Two-way ANOVA tests conducted with Tukey's multiple comparison test determined significant differences between tanδ values in "in-vivo 15min" below 400 Hz (see Table 4.3) as well as in "reperfusion 15min" and "reperfusion 1hr15min" predominantly at frequencies below 800 Hz (see Table 4.4 and Table 4.5). Significant differences were also found at "reperfusion 3hrs15min" and "reperfusion 4hrs14min" below 400 Hz (see Table 4.6 and Table 4.7). No significant differences in tanδ between groups were found at the end of NMP.

Frequency [Hz]	Compared Groups	Mean Diff.	95% CI of diff.	Adjusted P Value
398.107	Control vs. SCS	-1.898	-3.793 to -0.002	* 0.050
251.189	Control vs. SCS	-2.050	-3.637 to 0.179	* 0.025
199.526	Control vs. SCS	-1.875	-3.638 to -0.112	* 0.043
158.489	Control vs. SCS	-1.845	-3.416 to -0.274	* 0.033
125.892	Control vs. SCS	-1.810	-3.266 to -0.354	* 0.028
100.000	Control vs. SCS	-1.988	-3.645 to -0.330	* 0.031

Table 4.3: *Frequencies during "in-vivo 15min" where significant differences in tanδ are found between groups. * = P < 0.05.*

Frequency [Hz]	Compared Groups	Mean Diff.	95% CI of diff.	Adjusted P Value
1000000.000	Biliary Injury vs. SCS	0.5350	0.082 to 0.988	* 0.032
794.328	Control vs. SCS	-3.445	-5.807 to -1.083	* 0.018
630.957	Control vs. SCS	-4.698	-7.010 to -2.385	** 0.007
501.187	Control vs. SCS	-6.045	-8.871 to -3.219	** 0.006
398.107	Control vs. SCS	-7.348	-11.23 to -3.460	** 0.009
316.228	Control vs. SCS	-8.493	-13.74 to -3.247	* 0.014
251.189	Control vs. SCS	-9.295	-15.92 to -2.665	* 0.020
199.526	Control vs. SCS	-9.920	-17.97 to -1.871	* 0.029
158.489	Control vs. SCS	-10.25	-19.49 to -1.018	* 0.038
125.892	Control vs. SCS	-10.29	-20.54 to -0.037	* 0.050

Table 4.4: *Frequencies during "reperfusion 15min" where significant differences in tanδ are found between groups. * = P < 0.05 and ** = P < 0.01.*

Frequency [Hz]	Compared Groups	Mean Diff.	95% CI of diff.	Adjusted P Value
794.328	Control vs. SCS	-4.563	-10.97 to 12.08	* 0.016
630.957	Control vs. SCS	-5.690	-8.305 to -3.075	** 0.006
501.187	Control vs. SCS	-6.658	-9.388 to -3.927	** 0.004
398.107	Control vs. SCS	-7.448	-11.17 to -3.721	** 0.007
316.228	Control vs. SCS	-7.948	-12.98 to -2.918	* 0.014
251.189	Control vs. SCS	-8.113	-14.24 to -1.986	* 0.024
199.526	Control vs. SCS	-8.085	-15.25 to -0.922	* 0.036
158.489	Control vs. SCS	-7.795	-15.57 to -0.017	* 0.050
125.892	Biliary Injury vs. SCS	-5.953	-11.83 to -0.076	* 0.050
100.000	Biliary Injury vs. SCS	-5.393	-10.66 to -0.123	* 0.050

Table 4.5: *Frequencies during "reperfusion 1hr15min" where significant differences in tanδ are found between groups. * = P < 0.05 and ** = P < 0.01.*

Frequency [Hz]	Compared Groups	Mean Diff.	95% CI of diff.	Adjusted P Value
100000.000	Control vs. SCS	0.07650	0.030 to 1.500	* 0.050
316.228	Biliary Injury vs. SCS	-5.963	-11.87 to -0.051	* 0.050

Table 4.6: *Frequencies during "reperfusion 3hrs15min" where significant differences in tanδ are found between groups. * = P < 0.05 and ** = P < 0.01.*

Frequency [Hz]	Compared Groups	Mean Diff.	95% CI of diff.	Adjusted P Value
316.228	Biliary Injury vs. SCS	-4.303	-8.381 to -0.224	* 0.044
251.189	Biliary Injury vs. SCS	-3.965	-7.061 to -0.870	* 0.026
199.526	Biliary Injury vs. SCS	-3.655	-6.030 to -1.280	* 0.016
158.489	Biliary Injury vs. SCS	-3.248	-5.003 to -1.492	** 0.009
125.892	Biliary Injury vs. SCS	-2.845	-4.081 to -1.609	** 0.005
100.000	Biliary Injury vs. SCS	-2.455	-3.289 to -1.621	** 0.002

Table 4.7: *Frequencies during "reperfusion 4hrs15min" where significant differences in tanδ are found between groups. * = P < 0.05 and ** = P < 0.01.*

4.4 Tanδ max

Figure 4.8 shows the time development of maximum tanδ values during the experiment and are represented as the mean of each group with error bars with CI 95 %. To the left we see the time development of tanδm itself, whilst we see the time development of the frequency of tanδm to the right. The tanδm values (left) of the SCS group are seen to have a considerably decreased amplitude at "reperfusion 15min" and "reperfusion 1hr15min" compared to the other groups. The frequency of the tanδm values (right) are found at a higher frequency throughout the entire reperfusion protocol compared to the biliary injury and control groups.
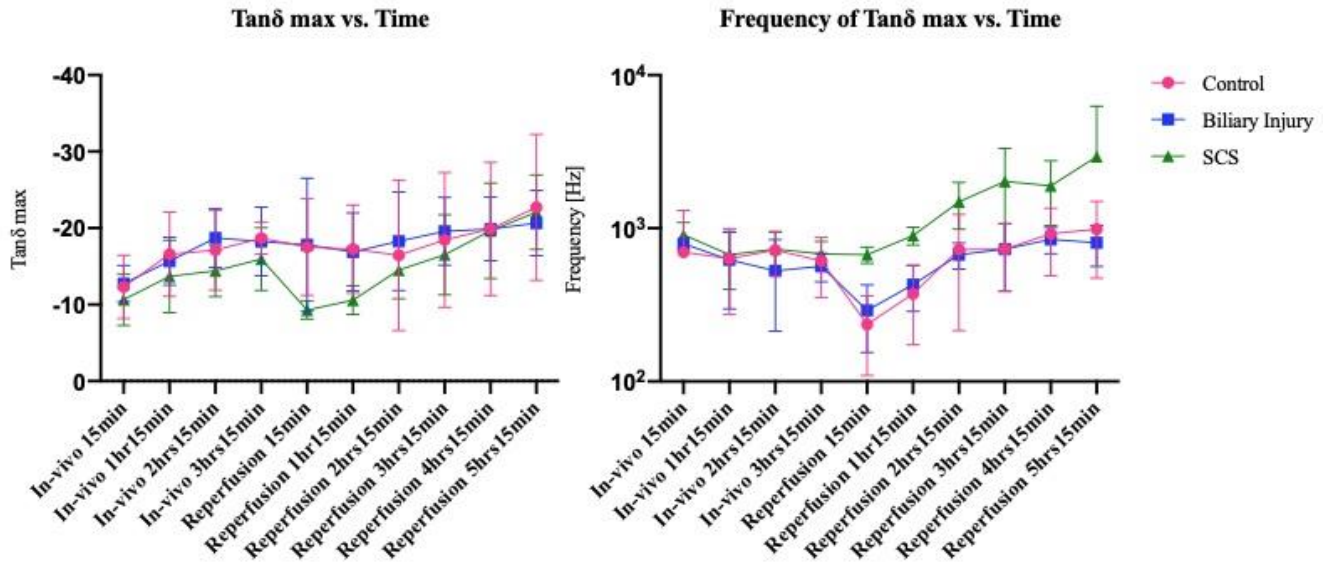
Figure 4.8: *Mean tanδm with CI 95 % vs. time. Left: tanδm vs. time. Right: frequency at which tanδm was measured vs. time.*

Two-way ANOVA with Tukey's multiple comparison test shows significant differences in tanδm between control and SCS groups at the first two time-intervals of reperfusion, see Figure 4.9 and Table 4.8.
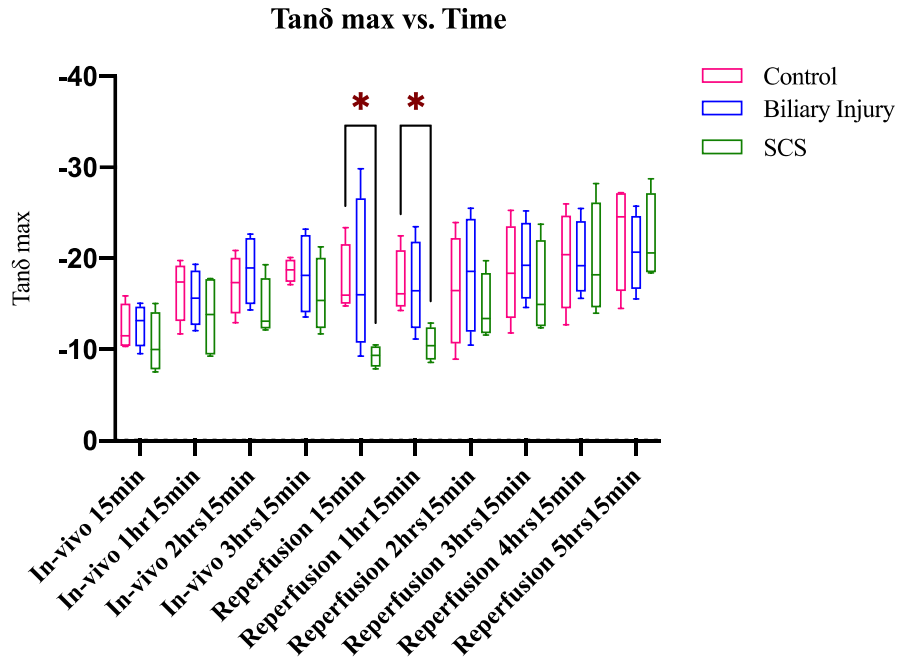
Figure 4.9: *Grouped box plot of tanδm vs. time. Boxes show mean and interquartile range while whiskers represent upper and lower range of measurement. * = P < 0.05.*

Time	Compared Groups	Mean Diff.	95% CI of diff.	Adjusted P Value
Reperfusion 1hr	Control vs. SCS	-8.245	-15.28 to -1.208	* 0.033
Reperfusion 2hrs	Control vs. SCS	-6.680	-11.65 to -1.705	* 0.023

Table 4.8: *Times where significant differences in tanδm are found between groups.*

* = P < 0.05.

Further significant differences were found comparing the frequency of tanδm between groups. Significant differences between the SCS group and the two remaining groups were found at "reperfusion 15min" and "reperfusion 1hr15min", see Figure 4.10 and Table 4.9.
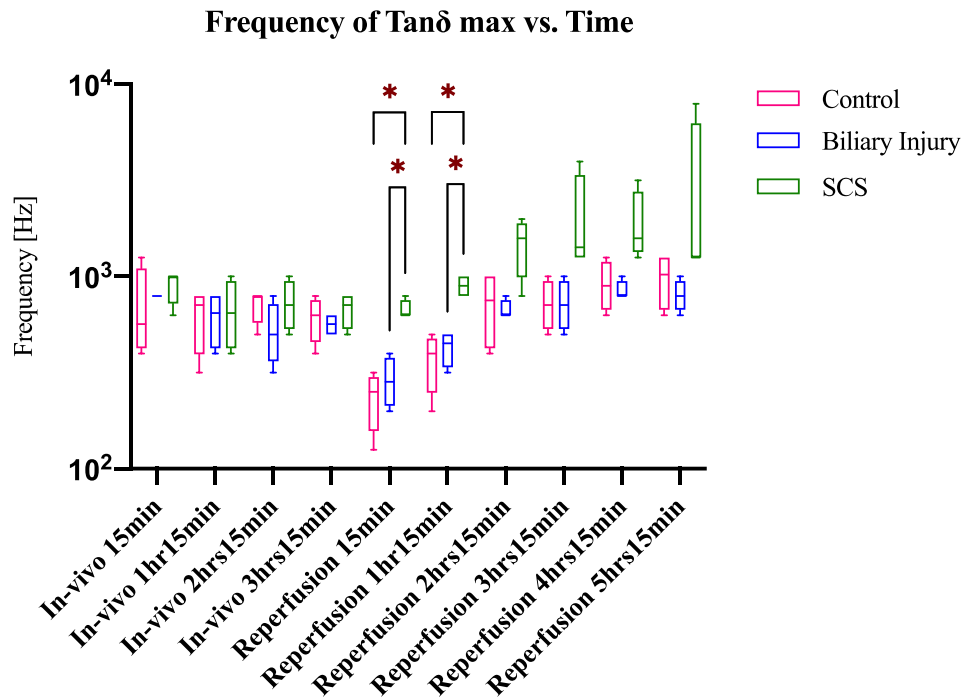
Figure 4.10: *Grouped box plot of frequency of where tanδm was measured vs. time. Boxes show mean and interquartile range while whiskers represent upper and lower range of measurement. * = P < 0.05.*

Time	Compared Groups	Mean Diff.	95% CI of diff.	Adjusted P Value
Reperfusion 1hr	Control vs. SCS	-435.7	-766.2 to -105.2	* 0.024
	Biliary Injury vs. SCS	-380.5	-663.9 to -97.19	* 0.023
Reperfusion 2hrs	Control vs. SCS	-522.9	-922.5 to -123.4	* 0.024
	Biliary Injury vs. SCS	-468.0	-895.6 to -40.41	* 0.040

Table 4.9: *Times where significant differences in frequency of tanδm are found between groups. * = P < 0.05.*

Chapter 5: Discussion

The objective of this study was to investigate the possibility of using bioimpedance measurements to determine the level of IRI in marginalised livers upon machine perfusion. Two marginalised liver groups (SCS and biliary injury) were investigated and compared with a control group by analysing $|Z|$, φ and $\tan\delta$. All of which are electrical parameters that amplify variations and relationships found in the raw data measured, namely the reactance and resistance.

5.1 Experiment Setup and Data Quality

The Ag/AgCl electrodes were the electrodes that proved most promising in the electrode test phase. The electrodes have a large surface area and the material properties of the Ag/AgCl result in a behaviour where current can flow at very low voltages, resulting in the lowest contribution from EPI of the two-electrode setups. The Ag/AgCl electrodes showed lower sensitivity to pressure changes than the other electrode setups and were well suited for potential electromagnetic noise in the operating room. Taking into account the heterogenous structure of the liver, the size and surface structure of the Ag/AgCl electrodes also allowed for greater area coverage and an even polarization distribution in the tissue of interest. Even though the contribution from EPI (< 1 kHz) was very low in amplitude, we estimate that there might be some EPI related noise that should be taken into account when interpreting the measurements below 1 kHz. Due to the stray inductance of the setup, there was also some noise at very high frequencies approximate to 1 MHz. Prior to and between measurements, electrodes were submerged in saline solution (0.9%) to reduce drift associated with the wet tissue interface and EPI.

A limitation with the selected electrode setup was that the design itself allowed for some variation in thickness of the liver tissue that was placed between the electrodes. While the liver lobes varied in structure and size, we tried to place the electrodes at similar locations with similar lobe thicknesses. The variation between pigs in liver lobe structures combined with variation in electrode placement probably led to increased variation in measured impedance,

while having less effect on the relationship parameters (φ and tanδ). Another limitation with the electrode setup was that we observed some corrosion between the metal grips of the electrode holders and the electrodes when the electrodes were left in the holders over time between experiments. To avoid this being an issue we tested the electrode setup before each experiment, by measuring the short impedance, where a threshold was set for acceptable measured resistance $\leq 0.3\Omega$. This allowed us to assess that the innate resistance and stray properties of the electrode setup was low and when needed led us to replace the electrode holder and then validate that the replacement did not have any sizeable influence on the results. The electrodes themselves were replaced for each experiment.

The datasets proved to be fairly consistent within each group (control, biliary injury and SCS), and the measured changes in electrical parameters within each group have followed the same tendencies throughout the study. As the datasets consisted of three groups containing an equal number of measurements ($n = 4$), the two-way ANOVA test was chosen to fit the datasets to statistically compare variance between groups to the variance within each group (S. Grimnes & Martinsen, 2017) (see analysis test variables in Chapter 3, section 3.6.1). We found no significant differences between groups when analysing the changes over time in |Z| but observed that the time trends in the different groups were somewhat similar. The variation in |Z| combined with a low number of observations probably affected the ability to discern between groups. Still, we could observe trends in the time-development of |Z| that are associated with expected patterns during ischemia (see section 5.2.1). We found there to be time-dependent significant differences between the factors in the datasets investigating φ, tanδ and tanδm which will be discussed further in sections 5.2.2 and 5.2.3.

Worth mentioning with respect to the results from the statistical analysis is the limitation of having a low sample size in each group ($n = 4$). SD is inversely proportional to the sample size, consequently we will see a greater margin of error in the statistical analysis with a small sample size. Each experiment lasted longer than 16 hours from start to finish, and was conducted every one to two weeks, depending on logistics regarding operating rooms and medical staff. While the DHOPE-COR-NMP trial at Oslo University Hospital consists of 24 pig experiments in addition to three pilot experiments, the time constraint for this study limited the number of experiments to a total of 12 pigs in addition to the pilot experiments.

5.2 Electrical Parameters of the Liver

5.2.1 Impedance Modulus

Figure 4.2 shows a large increase in amplitude of |Z| during "reperfusion 15min" and "reperfusion 1hr15min" across all groups. The increase in |Z| can be explained by multiple factors, the main one being cellular swelling caused by interruption in blood flow. The anaerobic metabolism and malfunctioning of the sodium-potassium membrane pump (see Chapter 2, section 2.2.2), causes depolarization of the cells leading to cellular swelling through osmosis. The narrowing of extracellular pathways impedes current in the lower frequency range as illustrated in Chapter 2, Figure 2.1. When applying this theory to in-vivo measurements of the biliary injury group we do not observe a rise in amplitude of |Z|. This might be due to the fact that the liver was not undergoing full warm ischemia, but rather becoming partially hypoxic. In order to damage the biliary tree, the hepatic artery was occluded in-vivo, however being an organ with dual blood supply, the liver still received nutrient rich blood containing usable levels of oxygen from the portal vein. We believe blood supply was sufficient for the cells of the liver lobes to remain viable throughout the duration of in-vivo measurements in the biliary injury group.

In addition to cellular swelling, lack of blood and decrease in temperature are contributing factors to the rise in amplitude of |Z| in the first two hours of reperfusion. Blood has resistivity of 100 - 200 $\Omega \cdot cm$, whilst liver tissue itself has resistivity averaging at 700 - 800 $\Omega \cdot cm$ at frequencies below 10 kHz (Haemmerich et al., 2002). Accordingly, blood acts as a conductor of current in the liver tissue when present. At frequencies below 10 kHz the difference between resistivity of the blood and liver tissue is much higher than at high frequencies, resulting in greater variation in measurements in the low frequency range (Haemmerich et al., 2002). This is most noticeable in the first measurement of reperfusion where blood is not present, see Figure 4.3. The changes in |Z| observed during reperfusion further supports Foster's findings correlating a gradual increase in tissue conductivity with a gradual increase in temperature up to 37°C in frequencies below 1 GHz (Foster & Schwan, 1989).

5.2.2 Phase

Significant differences in φ between the SCS group and control group were observed in the same frequency range for measurements at "reperfusion 15min" and "reperfusion 1hr15min". At "reperfusion 15min" we found $P = 0.005$ at frequency 200 Hz, whilst at "reperfusion 1hr15min" we found $P = 0.0007$ at the same frequency point, indicating very to extremely significant differences in the low frequency range. The phase-shifts observed in the different stages of the experiment (in-vivo, start and end of reperfusion) are proportional to changes in X_C (nominator) and R (denominator). The increased amplitude of φ in the SCS group in the frequency range 100 Hz to 1 kHz indicate a change in X_C and/or R differing from control. From analysis of the raw data, we observed an increase in R and a decrease in the capacitive components of X at frequencies below 1 kHz between the SCS group and the control group. The amplitude of the R values was subject to a high margin of error between pigs. As R is considered an equivalent series resistance describing the sum of ohmic losses, we suspect that the margin of error is correlated to the width of the lobe and consequently the distance between the electrodes. The low-frequency increased resistance corresponds with IRI related to cellular swelling (see Chapter 2, section 2.2.2) effectively narrowing the extracellular current path. The amplitude of the X_C values stayed consistent between pigs, and the low-frequency decrease of the capacitive properties compared to the control group corresponds with IRI where cells are unable to uphold the ion potential across the membranes due to cellular swelling by osmosis. This in turn increases the cell permeability and lowers the cell membrane capacitance. We know the endothelial cells in particular are subject to apoptosis and necrosis following prolonged cold storage (Klune & Tsung, 2010), and we assume the phase-shift observed upon reperfusion is in correlation with damaged endothelial cells. As the phase ratio of SCS could also be influenced by the fact that the liver was in cold storage overnight and perhaps being colder in temperature than the control livers, we looked up the liver temperature measured with the pCO2 sensors in the liver parenchyma. The temperature 15 minutes into reperfusion was $11°C \pm 1°C$ regardless of the group, indicating that the difference in φ at low frequencies is an indication of physical changes caused by ischemia and was not caused by temperature differences in the tissue at the time of measurement.

5.2.3 Tanδ and Tanδ max

When comparing tanδ measurements between groups in "reperfusion 15min" and "reperfusion 1hr15min" we observed a decreased amplitude of tanδ in the SCS group and increased amplitude in the control group, with significant differences in the frequency range 100 - 800 Hz. Among these we found P = 0.006 for "reperfusion 15min" and P = 0.004 for "reperfusion 1hr15min" at a frequency of 501 Hz, indicating very significant differences in the low frequency range. We also found some statistical differences between the SCS group and the control group in the "in-vivo 15min" time-interval. We did not expect to see any differences in this interval and assume that the natural variance in livers from pig to pig, combined with the small sample size, affect the analysis, as mentioned in section 5.1.

When investigating tanδm over time, the tangent of the ratio between R and X_C appears to be sensitive to ischemia with significant difference between the control group and the SCS group in the first two hours of reperfusion (P = 0.033 for "reperfusion 15min" and P = 0.023 for "reperfusion 1hr15min"). As X_C is the denominator in tanδ, the relationship between the impedance components amplifies the capacitive changes we observed in φ. This was again validated when analysing the time development of the frequency of tanδm (P = 0.024 for "reperfusion 15min" and P = 0.024 for "reperfusion 1hr15min"). We also found significant differences in frequency of tanδm in the first two time-intervals of reperfusion between the SCS group and the biliary injury group. As discussed in section 5.2.1, we assume these findings have to do with the dual blood supply of the liver, as the electrical behaviour of the biliary injury group proved similar to the control group for all parameters.

Strand-Amundsen et al. (2018) reported an initial increase in the amplitude of tanδm in the first hours of reperfusion in pig small intestine, with the control tissue measurements measured at a higher amplitude than the ischemic tissue measurements, following a higher increase in tanδm later on in the reperfusion stage. This trend is observed in our findings (see Figure 4.9) although no significant difference was found when comparing groups at the later stages of reperfusion. When looking at the frequency of tanδm in the reperfusion stage we observe a similar increasing trend as with the tanδm values, but with the SCS group measurements measured at a higher frequency than the control

group throughout the reperfusion stage (see Figure 4.10). Figure 4.9 and Figure 4.10 indicate that there is a late change in the relationship between R and X, but there was also a large variation in these four measurements, so no significant difference was observed. In addition to endothelial cells being susceptible to apoptosis and necrosis, we know long duration cold storage introduces increased activation of Kupffer cells during reperfusion. Kupffer cells produce ROS and increases cytokine production which exacerbates IRI (Klune & Tsung, 2010) (see Chapter 2, section 2.2.2). The extent of damaged cells and necrotic tissue is yet to be assessed by the pathologist; thus, we are not certain of the exact mechanisms that causes the electrical properties of the liver tissue measured over the lobe in the different groups to become more similar after some hours of reperfusion with warm blood. Other parameters such as low gall production, inadequate lactate metabolism and high glucose consumption indicated overall low viability of the SCS livers at the end of NMP, however these parameters still remain to be subject to statistical analysis. In the surgeon's experience, a small proportion of livers being subjected to cold storage between approximately 15 - 20 hours can fully recover upon reperfusion, meaning IRI is reversed. Whether reversible effects are the cause of no significant differences found in φ or tanδ at the end of NMP will have to be assessed when the histopathological analysis has been made available.

5.2.4 Summary of Findings

Based on discussion of quality of data and consistent significant differences ($P < 0.01$) found in φ and tanδ at low frequencies (< 800 Hz) between the SCS group and control group, we reject the null hypothesis at two time-intervals: "reperfusion 15min" and "reperfusion 1hr15min".

5.3 Limitations

Due to this study being part of a larger project establishing the DHOPE-COR-NMP protocol for future liver transplantations at the Oslo University Hospital, the project is still ongoing. Although tissue samples were taken regularly throughout the experiments, the histological analysis is not yet available. A comparison of changes in electrical properties with histological assessment of the same tissue could have been of great value to evaluate significant differences between groups as well as to link electrical behaviour with pathophysiological changes in the liver tissue.

The porcine liver is genetically close to human liver, and though the shape and size of the liver lobes are different, the functionality and anatomy including vascular and biliary structures share common structures (Nykonenko, Vávra, & Zonča, 2017). While the SCS group show significant difference from the control group indicating IRI, the model of in-vivo induced biliary injury remains fairly uncertain in our results and need further investigation prior to assuming translation of results equating biliary injury in a human liver. The medical team that is part of this project is still waiting for feedback from the pathologist, before the injury level in the partially occluded liver (biliary injury) can be realistically assessed. As we measured on the liver lobe, we estimate not to find much injury in the tissue in the biliary injury group, as the partial perfusion should be sufficient to keep the parenchymal liver cells alive.

This study was conducted over the course of the SARS-CoV-2 pandemic, with Oslo city being in lockdown for the majority of the thesis. Taking place in a hospital, this project has been subjected to delays and logistical challenges regarding medical staff and booking of operating rooms due to the pandemic. Health and safety measures, with all that it entails, has been part of the study process in this novel period in time.

Chapter 6: Conclusion

Oslo University Hospital is incorporating machine perfusion of donor livers with the objective to increase the numbers of organs suitable for transplantation. This master thesis has focused on investigating the possibility of using bioimpedance as a way of contributing to the assessment of the level of IRI displayed by two groups of marginalised livers (SCS and biliary injury) upon machine perfusion.

We have found that the electrical ratio parameters φ and $\tan\delta$ are sensitive to changes in the tissue caused by ischemia and reperfusion, and that the difference between the means of the groups (control, biliary injury and SCS) are significantly different at certain intervals in the time duration of the experiment.

Bioimpedance measurement on the liver lobe for the biliary injury group did not measure significant differences from the control group as we conclude the liver parenchyma received sufficient blood flow from the portal vein during the occlusion of the hepatic artery. We could not predict partial liver hypoxia in the liver parenchyma based on this model.

We found significant differences in the time-development of passive electrical properties between long duration ischemia in the SCS group and short duration ischemia in the control group. Given that we know the time since liver explanation, this means it is possible to use bioimpedance measurements in the intervals where the differences between the groups are significant, to discriminate the state of the liver in real-time. We conclude that we can differentiate between the SCS group and control group in in the DHOPE and COR stage of the machine perfusion protocol.

Though significant differences were established at the start of reperfusion for the SCS group, based on the measurement data we cannot predict irreversible effects of IRI in the marginalised liver model at the end of NMP.

6.1. Future Work and Perspectives

We believe bioimpedance to be a potentially promising non-invasive tool to aid surgeons in real-time IRI assessment of organs upon machine perfusion, with the aim to discard of fewer marginalised donor livers. We especially encourage further investigation into the electrical parameters during NMP. However, a lot of work remains for it to be considered a reliable tool in liver viability assessment. For future work we have listed a few suggestions:

1. We believe further investigation into the electrical properties of the gall duct could be valuable, albeit challenging, in order to determine categorization of IRI in marginalised livers with damaged biliary structures.

2. Combine assessment of IRI with histological samples to further establish change in electrical properties in tissue with the pathophysiological changes.

3. Development of electrode system with software simulated model (e.g.: COMSOL Multiphysics®) for estimation of sensitivity area.

4. Bioimpedance measurements on human livers to compare results with porcine liver and assess the translational value.

References

Ahn, H., Shin, H., Yun, S., Kim, J., & Choi, J. (2005). Measurement of bioimpedance and cell viability during ischemia-reperfusion in the rat liver. *Conf Proc IEEE Eng Med Biol Soc, 2005*, 1945-1947. doi:10.1109/iembs.2005.1616833

Al-Surkhi, O. I., & Naser, R. Y. (2018). Detection of Cell Morphological Changes of Ischemic Rabbit Liver Tissue Using Bioimpedance Spectroscopy. *IEEE Transactions on NanoBioscience, 17*(4), 402-408. doi:10.1109/TNB.2018.2853269

Albulbul, A. (2016). Evaluating Major Electrode Types for Idle Biological Signal Measurements for Modern Medical Technology. *Bioengineering, 3*, 20. doi:10.3390/bioengineering3030020

Czigany, Z., Lurje, I., Schmelzle, M., Schöning, W., Öllinger, R., Raschzok, N., . . . Lurje, G. (2020). Ischemia-Reperfusion Injury in Marginal Liver Grafts and the Role of Hypothermic Machine Perfusion: Molecular Mechanisms and Clinical Implications. *J Clin Med, 9*(3). doi:10.3390/jcm9030846

Foster, K., & Schwan, H. P. (1989). Dielectric properties of tissues and biological materials: A critical review. *Critical reviews in biomedical engineering, 17*, 25-104.

Geddes, L. A., & Baker, L. E. (1967). The specific resistance of biological material—A compendium of data for the biomedical engineer and physiologist. *Medical and biological engineering, 5*(3), 271-293. doi:10.1007/BF02474537

Gersing, E. (1998). Impedance spectroscopy on living tissue for determination of the state of organs. *Bioelectrochemistry and Bioenergetics, 45*(2), 145-149. doi:https://doi.org/10.1016/S0302-4598(98)00079-8

Gordillo, M., Evans, T., & Gouon-Evans, V. (2015). Orchestrating liver development. *Development, 142*(12), 2094. doi:10.1242/dev.114215

Grimnes, S., & Martinsen, Ø. (2010). Alpha-dispersion in human tissue. *Journal of Physics: Conference Series, 224*, 012073. doi:10.1088/1742-6596/224/1/012073

Grimnes, S., & Martinsen, Ø. G. (2017). *Bioimpedance & Bioelectricity Basics* (Vol. 3rd): Elsevier Academic Press.

Haemmerich, D., Ozkan, O. R., Tsai, J. Z., Staelin, S. T., Tungjitkusolmun, S., Mahvi, D. M., & Webster, J. G. (2002). Changes in electrical resistivity of swine liver after occlusion and postmortem. *Medical and Biological Engineering and Computing, 40*(1), 29-33. doi:10.1007/BF02347692

Hagness, M., Foss, S., Sørensen, D. W., Syversen, T., Bakkan, P. A., Dahl, T., . . . Line, P. (2019). Liver Transplant After Normothermic Regional Perfusion From Controlled Donors After Circulatory Death: The Norwegian Experience. *Transplant Proc, 51*(2), 475-478. doi:10.1016/j.transproceed.2019.01.066

Hernández-Balaguera, E., López-Dolado, E., & Polo, J. L. (2016). Obtaining electrical equivalent circuits of biological tissues using the current interruption method, circuit theory and fractional calculus. *RSC Advances, 6*(27), 22312-22319. doi:10.1039/C5RA24535D

Ishai, P., Talary, M., Caduff, A., Levy, E., & Feldman, Y. (2013). TOPICAL REVIEW Electrode polarization in dielectric measurements: a review. *Measurement Science and Technology, 24*, 102001-102021. doi:10.1088/0957-0233/24/10/102001

Kalogeris, T., Baines, C. P., Krenz, M., & Korthuis, R. J. (2012). Cell biology of ischemia/reperfusion injury. *Int Rev Cell Mol Biol, 298*, 229-317. doi:10.1016/B978-0-12-394309-5.00006-7

54

Klune, J. R., & Tsung, A. (2010). Molecular Biology of Liver Ischemia/Reperfusion Injury: Established Mechanisms and Recent Advancements. *Surgical Clinics of North America, 90*(4), 665-677. doi:https://doi.org/10.1016/j.suc.2010.04.003

Melum, E. (2020). *The Nordic Liver Transplant Registry (NLTR) Annual report 2019*. Retrieved from http://www.scandiatransplant.org/resources

Mergental, H., Laing, R. W., Kirkham, A. J., Perera, M., Boteon, Y. L., Attard, J., . . . Mirza, D. F. (2020). Transplantation of discarded livers following viability testing with normothermic machine perfusion. *Nat Commun, 11*(1), 2939. doi:10.1038/s41467-020-16251-3

Miklavcic, D., Pavselj, N., & Hart, F. (2006). Electric Properties of Tissues. In (Vol. 6).

Muller, X., Schlegel, A., Kron, P., Eshmuminov, D., Würdinger, M., Meierhofer, D., . . . Dutkowski, P. (2019). Novel Real-time Prediction of Liver Graft Function During Hypothermic Oxygenated Machine Perfusion Before Liver Transplantation. *Ann Surg, 270*(5), 783-790. doi:10.1097/sla.0000000000003513

Naranjo-Hernández, D., Reina-Tosina, J., & Min, M. (2019). Fundamentals, Recent Advances, and Future Challenges in Bioimpedance Devices for Healthcare Applications. *Journal of Sensors, 2019*, 9210258. doi:10.1155/2019/9210258

Nykonenko, A., Vávra, P., & Zonča, P. (2017). Anatomic Peculiarities of Pig and Human Liver. *Exp Clin Transplant, 15*(1), 21-26.

Rijn, R., Karimian, N., Matton, A., Burlage, L., Westerkamp, A., Berg, A., . . . Porte, R. (2016). Dual hypothermic oxygenated machine perfusion in liver transplants donated after circulatory death grafts. *The British journal of surgery, 99*, 85-86. doi:10.1002/bjs.10515

Strand-Amundsen, R. J., Tronstad, C., Kalvøy, H. v., Ruud, T. E., Høgetveit, J. O., Martinsen, r. G. t., & Tønnessen, T. I. (2018). Small intestinal ischemia and reperfusion - Bioimpedance measurements. *Strand-Amundsen, Runar J. (2019) Assessment of small intestinal viability: A bioimpedance approach. Doctoral thesis http://hdl.handle.net/10852/67667*.

van Leeuwen, O. B., de Vries, Y., de Meijer, V. E., & Porte, R. J. (2021). Hypothermic machine perfusion before viability testing of previously discarded human livers. *Nat Commun, 12*(1), 1008. doi:10.1038/s41467-021-21182-8

Williams, W. W., & Markmann, J. F. (2021). Warming Up to Cold Perfusion. *N Engl J Med*. doi:10.1056/NEJMe2102056

Yang, L. L. (2021). Anatomy and Physiology of the Liver. In Z. Milan & C. Goonasekera (Eds.), *Anesthesia for Hepatico-Pancreatic-Biliary Surgery and Transplantation* (pp. 15-40). Cham: Springer International Publishing.

Zhai, Y., Petrowsky, H., Hong, J. C., Busuttil, R. W., & Kupiec-Weglinski, J. W. (2013). Ischaemia-reperfusion injury in liver transplantation--from bench to bedside. *Nature reviews. Gastroenterology & hepatology, 10*(2), 79-89. doi:10.1038/nrgastro.2012.225